

PRECONDITIONED ACCELERATED GRADIENT DESCENT METHODS FOR LOCALLY LIPSCHITZ SMOOTH OBJECTIVES WITH APPLICATIONS TO THE SOLUTION OF NONLINEAR PDES

JEAN-HYUN PARK, ABNER J. SALGADO, AND STEVEN M. WISE

ABSTRACT. We analyze preconditioned Nesterov’s accelerated gradient descent methods (PAGD) for approximating the minimizer of locally Lipschitz smooth, strongly convex objective functionals. To facilitate our analysis, we introduce a second-order ordinary differential equation (ODE) and demonstrate that this ODE is the limiting case of PAGD as the step size tends to zero. Using a simple energy argument, we show an exponential convergence of the ODE solution to its steady state. The PAGD method may be viewed as an explicit-type time-discretization scheme of the ODE system, which requires a natural time step restriction for energy stability. Assuming this restriction, an exponential rate of convergence of the PAGD sequence is demonstrated, by mimicking the convergence of the solution to the ODE via energy methods. Application of the PAGD method is made in the context of solving certain nonlinear elliptic PDE using pseudo-spectral methods, and several numerical experiments are conducted. The results confirm the global geometric and h -independent convergence of the PAGD method, with an accelerated rate that is improved over the preconditioned gradient descent (PGD) method.

1. INTRODUCTION

The purpose of this work is to shed some light on the convergence properties of a very well-known and efficient algorithm for unconstrained convex minimization: the so-called Nesterov’s accelerated gradient descent (AGD) scheme. This method attempts to iteratively find approximations to the following problem: given $G : \mathbb{H} \rightarrow \mathbb{R}$, find

$$x^* = \operatorname{argmin} \{G(x) \mid x \in \mathbb{H}\}.$$

Here, and in what follows, \mathbb{H} is a separable and real Hilbert space with inner product $(\cdot, \cdot)_{\mathbb{H}}$ and the so-called *objective* functional G is assumed to be strongly convex and locally Lipschitz smooth; see Section 2 for definitions and notation. We immediately comment that the assumptions on the objective guarantee the existence and uniqueness of a minimizer [10, Theorem 7.4-4, Theorem 8.2-2].

Convex minimization is ubiquitous, and our main interest in this problem comes from the fact that many important nonlinear partial differential equations (PDE) can be viewed as the Euler equations of certain convex objective functions, e.g., the classical minimal surface problem [12] and the p -Laplacian equation [3] have this structure. In a related context, the current boom of statistical learning has

2010 *Mathematics Subject Classification.* 65B99, 65J08, 65N35, 65K10.

Key words and phrases. Preconditioning, Nesterov Acceleration, Momentum Method, Convex Optimization, Nonlinear Elliptic Partial Differential Equations, Pseudo-Spectral Methods.

drawn the interest of practitioners to so-called first order schemes, i.e., those that only require knowledge of first order derivatives since they make it suitable to deal with large data. These considerations are important for solving nonlinear PDE as well. One of the main thrusts of this research is to show that Nesterov's accelerated schemes, which are popular in statistical learning, can be utilized as fast solvers for nonlinear PDE.

The first and most naïve approach to find x^* would be to appeal directly to the first order necessary (and in this context sufficient) optimality condition, that is, the Euler equation

$$(1.1) \quad G'(x^*) = 0,$$

where G' denotes the Fréchet derivative of G . In the examples that we have in mind, however, this requires the simultaneous solution to a very large number of nonlinear equations, and this is not feasible in practice. Other approaches better suited for minimization must be constructed. According to [5], iterative methods for minimizing functionals date back in 1847 when Cauchy proposed the so-called gradient descent method (GD). The solution to (1.1) can be seen as the steady state of the *gradient flow*

$$(1.2) \quad X(0) = x_0, \quad \dot{X}(t) = -G'(X(t)), \quad t > 0.$$

Here $x_0 \in \mathbb{H}$ is arbitrary and, in the second equation, we are implicitly identifying the dual space of \mathbb{H} , denoted by \mathbb{H}' , with \mathbb{H} itself. Under the assumptions we have imposed on the objective G , it is possible to show that this flow satisfies $X(t) \rightarrow x^*$ as $t \rightarrow \infty$, see [22, Theorem 2.4]. The idea of GD is to approximate the solution to this flow via a *forward Euler* time discretization with a fixed step size s : given $x_0 \in \mathbb{H}$, for $k \geq 0$, find x_{k+1} satisfying

$$(1.3) \quad x_{k+1} = x_k - sG'(x_k).$$

While this idea seems straightforward, more in-depth discussions on this method started only in the 1960s, where some practical step size rules and convergence analyses were established. It was shown that if the objective functional is convex and Lipschitz smooth, then GD converges to the minimizer, x^* , and it exhibits a first order rate of convergence in the objective. Here and in what follows, by an *n -th order (algebraic) convergence* in the objective, we mean that $G(x_k) - G^* \leq O(1/k^n)$ as $k \rightarrow \infty$ and by an *exponential* or a *geometric convergence* in the objective that $G(x_k) - G^* \leq O(r^k)$ as $k \rightarrow \infty$ for some $r \in (0, 1)$, where $G^* = G(x^*)$ is the minimum of G . In the latter case, we call r the rate of (exponential) convergence. It can further be shown that if the objective is, in addition, strongly convex, then the rate of convergence is exponential, and that it matches the rate of convergence of the solution of (1.2) to x^* (see [17, Theorem 2.1.15] or Remark 5.11). Some physical intuition for the evolution of the solution to (1.2) is provided in Section 4. See, in particular, Remark 4.1.

To improve the convergence rate of GD, in 1983, Nesterov [16] suggested a scheme that accelerates the GD method. For convex and Lipschitz smooth objectives the Nesterov's accelerated gradient descent (AGD) scheme achieves a second order convergence rate. Later, in [17, Theorem 2.1.15], he showed that if the objective is, in addition, strongly convex, then AGD achieves a faster exponential convergence rate than GD.

However, while the GD scheme has a strong physical intuition behind it, it is not completely clear what mechanism is at play to provide an acceleration in the AGD scheme. Some attempts in this direction were made [2, 22, 21]. For instance, using an ODE approach, Su et al. [21] were able to explain the acceleration from first to second order for convex, Lipschitz smooth objectives. However, that framework does not explain the exponential acceleration for the better-behaving class of objectives that we are interested in here: those that are, in addition, strongly convex. The model of [21] will play an important role in our discussion, and we provide additional details about it in Section 4.

Evidently, all considerations regarding convergence are subject to the norm $\|\cdot\|_{\mathbb{H}}$. It is possible to improve the convergence rate by using an equivalent norm, through which the level sets of the objective G look “more circular” than other ones. In the linear algebra setting this is commonly known as *preconditioning*. In the context of (1.2) and GD, this is achieved by introducing an operator $\mathcal{L} : \mathbb{H} \rightarrow \mathbb{H}'$ and considering the evolution of $\dot{X}(t) = -\mathcal{L}^{-1}G'(X(t))$. Notice that we no longer implicitly identify \mathbb{H}' with \mathbb{H} . The time-discrete counterpart of (1.3) is known as the *preconditioned gradient descent method* (PGD) and is as follows: given $x_0 \in \mathbb{H}$, for $k \geq 0$, find x_{k+1} such that

$$x_{k+1} = x_k - s\mathcal{L}^{-1}G'(x_k).$$

If the preconditioner is suitably chosen, then the convergence rate of GD can be substantially improved [13]. Note that we will tacitly assume in the sequel that \mathcal{L} is independent of the iteration index k .

We remark that Newton’s method may be viewed as a kind of *generalized* preconditioned gradient descent method if we assume that G is twice Fréchet differentiable and allow for the possibility that the preconditioner can change at each iteration. In particular, Newton’s method is expressed as

$$G''(x_k)(x_{k+1} - x_k) = -G'(x_k) =: r_k,$$

where $G''(x_k)$ is the second Fréchet derivative of G , and r_k is the so-called residual. Then, Newton’s method is a generalized preconditioned gradient descent method for which the preconditioner satisfies $s\mathcal{L}_k = G''(x_k)$. One of the difficulties with Newton’s method is that the preconditioner constantly changes, in general, and must be recomputed and re-inverted at each iteration step, which can prove quite costly. Furthermore, G'' may not exist in all applications of interest. Indeed, in the sequel, we will not assume that G'' exists.

The work contained herein includes five important contributions to our understanding of PAGD.

1. We provide an intuitive explanation for the acceleration mechanism behind AGD for strongly convex and locally Lipschitz smooth objectives. This is achieved by studying a continuous-time counterpart, which, although inspired by [21], is novel and allows to extract additional information from the scheme. We view AGD as a discretization of a certain second order ordinary differential equation (ODE) — indeed, we present how to discretize this ODE to obtain AGD — and show that the solution to this ODE converges to its stationary point, which is the minimizer of G , exponentially fast.

2. We provide an *energy based* proof of the exponential convergence rate of AGD. This proof mimics the analysis of the continuous counterpart previously developed and shows what dissipation mechanisms are at play to achieve the aforementioned acceleration. We also show that the rates of convergence of the ODE model and AGD match.
3. We show, in an explicit way, that if the objective functional is locally Lipschitz smooth and strongly convex, then a preconditioned accelerated gradient descent scheme (PAGD) can be devised, and its performance is significantly improved when compared with AGD. This seems deceptively simple. After all, preconditioning is nothing but using a different norm, hence a numerical analysis in one norm implicitly suggests the possibility of a similar analysis in another norm. However, actually conducting the analysis that is implicitly expected and confirming the result by specifying a preconditioner needs work. We will do this job simultaneously with the first two purposes in the sense that we analyze an ODE and the related scheme where a preconditioner is built into their constructions.
4. We demonstrate that PAGD methods can be effectively and efficiently used to solve complicated nonlinear (and even nonlocal) elliptic PDE. In particular, under reasonable assumptions, the convergence rate is geometric and h -independent, where h is the spatial grid size. Generally, the rate of convergence for PAGD is $1 - \sqrt{\rho}$, where ρ is the h -independent nonlinear (inverse) condition number (defined below). Compare this to the rate of convergence for the PGD method, which is roughly $1 - \rho$. In other words, the speed-up is analogous to that observed using the conjugate gradient method for solving a linear SPD system instead of the steepest descent method. See Section 3 and Remark 5.11 for more details regarding the convergence rates.
5. Finally, we prove all of our results under the more general assumption that the objective function is locally Lipschitz. Most, if not all, earlier works assume that the objective is *globally Lipschitz* [17, 22, 21, 2], by contrast. This might seem like a trivial matter, after all, the considerations can always be confined to a sufficiently large neighborhood of the minimizer. However, in the applications that we have in mind (discretized PDEs), this is an important issue as we wish to prescribe parameters to our schemes and attain rates of convergence that have little or no dependence on h .

This paper is organized as follows. In Section 2, we summarize the notation, assumptions, and main tools that we will use. In Section 3, we introduce several numerical schemes that are closely related to our discussion and summarize their convergence rates. The first goal is achieved in Section 4, where we explore the connection between PAGD and a second order ODE and how this connection can help understand the acceleration behind PAGD intuitively. Section 5 is dedicated to our second goal. We prove the existence of an invariant set for the PAGD scheme and, more importantly, its exponential convergence. We take an ODE inspired approach, whose intuition lies in the developments of Section 4. In Section 6, we illustrate the application of the PAGD method to the solution of some numerical PDEs. These numerical experiments show the improvement in convergence by both acceleration and preconditioning. Finally, in Appendix A, we provide the derivation of the initial value problem (IVP) which corresponds to the limiting case of PAGD.

We must finally point out that, after the core of the analysis for this paper was completed, we became aware of [15], where an ODE model for AGD is also

derived. The model is quite similar to ours, and the authors of [15] also use it to obtain convergence of AGD via energy arguments. However, [15] assumes that the objective is *globally* Lipschitz smooth, and the effect of preconditioning is not taken into consideration. In contrast, [15] also considers other types of objectives, like merely convex ones. We believe that, although having similar results, both our works are complementary to each other.

2. PRELIMINARIES

Let us begin by introducing the setting, assumptions, and some basic properties of the objects that we are interested in. By \mathbb{H} , we denote a real and separable Hilbert space with inner product $(\cdot, \cdot)_{\mathbb{H}}$ and associated norm $\|\cdot\|_{\mathbb{H}}$. Since we will use other inner products and norms on \mathbb{H} , for clarity, we will refer to $(\cdot, \cdot)_{\mathbb{H}}$ and $\|\cdot\|_{\mathbb{H}}$ as the *canonical inner product* and *canonical norm*, respectively. The dual of \mathbb{H} is denoted by \mathbb{H}' . Its canonical operator norm is denoted by $\|\cdot\|_{\mathbb{H}'}$. For $v \in \mathbb{H}$ and $f \in \mathbb{H}'$, the symbol $\langle f, v \rangle$ represents their duality pairing, that is, $\langle f, v \rangle = f(v) \in \mathbb{R}$.

To incorporate the effect of preconditioning into our discussion, we introduce, following [13], a linear operator $\mathcal{L} : \mathbb{H} \rightarrow \mathbb{H}'$, which we call a *preconditioner*. Such an operator induces a bilinear form: for $x, y \in \mathbb{H}$,

$$(2.1) \quad (x, y)_{\mathcal{L}} = \langle \mathcal{L}x, y \rangle = \mathcal{L}[x](y).$$

We further assume that the bilinear form defined in (2.1) satisfies the following properties: there exist $C_1, C_2 > 0$ such that, for any $x, y \in \mathbb{H}$,

$$(2.2) \quad (x, y)_{\mathcal{L}} = (y, x)_{\mathcal{L}},$$

$$(2.3) \quad (x, y)_{\mathcal{L}} \leq C_2 \|x\|_{\mathbb{H}} \|y\|_{\mathbb{H}},$$

$$(2.4) \quad C_1 \|x\|_{\mathbb{H}}^2 \leq (x, x)_{\mathcal{L}}.$$

We will use the following well-known result:

Theorem 2.1 (Riesz representation). *Let \mathbb{H} be a Hilbert space with inner product $(\cdot, \cdot)_{\mathbb{H}}$, and suppose that $(\cdot, \cdot)_{\beta}$ is another inner product that is equivalent to $(\cdot, \cdot)_{\mathbb{H}}$, that is, their respective norms are equivalent. For any $f \in \mathbb{H}'$, there is a unique element $x_{\beta, f} \in \mathbb{H}$ satisfying*

$$(x_{\beta, f}, y)_{\beta} = \langle f, y \rangle, \quad \forall y \in \mathbb{H}.$$

Furthermore,

$$\|x_{\beta, f}\|_{\beta} = \sqrt{(x_{\beta, f}, x_{\beta, f})_{\beta}} = \sup_{\substack{x \in \mathbb{H} \\ \|x\|_{\beta} = 1}} \langle f, x \rangle.$$

The invertible, linear mapping $\mathfrak{R}_{\beta} : \mathbb{H}' \rightarrow \mathbb{H}$ defined by $\mathfrak{R}_{\beta}(f) = x_{\beta, f}$ is called the *Riesz map with respect to $(\cdot, \cdot)_{\beta}$* .

Let us state some immediate, but important consequences without proof for the sake of brevity.

Proposition 2.2 (properties of \mathcal{L}). *Let \mathbb{H} be a real and separable Hilbert space with inner product $(\cdot, \cdot)_{\mathbb{H}}$, and suppose that $\mathcal{L} : \mathbb{H} \rightarrow \mathbb{H}'$ is a linear mapping that satisfies (2.2)–(2.4). Then, $(\cdot, \cdot)_{\mathcal{L}}$ is an inner product on \mathbb{H} and the object*

$$\|x\|_{\mathcal{L}} = \sqrt{(x, x)_{\mathcal{L}}}, \quad \forall x \in \mathbb{H},$$

is a norm, which is, in fact, equivalent to the original norm, $\|\cdot\|_{\mathbb{H}}$. By the Riesz Representation Theorem, \mathcal{L} is invertible. The inverse is continuous and, in fact, it is just the Riesz Map with respect to the \mathcal{L} -inner product, denoted $\mathfrak{R}_{\mathcal{L}}$. We write $\mathcal{L}^{-1} = \mathfrak{R}_{\mathcal{L}} : \mathbb{H}' \rightarrow \mathbb{H}$. The object

$$(2.5) \quad (f, g)_{\mathcal{L}^{-1}} = \langle f, \mathcal{L}^{-1}g \rangle, \quad \forall f, g \in \mathbb{H}',$$

is an inner product on the Hilbert space \mathbb{H}' and the object

$$(2.6) \quad \|f\|_{\mathcal{L}^{-1}} = \sqrt{(f, f)_{\mathcal{L}^{-1}}} = \sqrt{\langle f, \mathcal{L}^{-1}f \rangle}, \quad \forall f \in \mathbb{H}',$$

is a norm. The new norm on \mathbb{H}' is an operator norm in the sense that

$$(2.7) \quad \|f\|_{\mathcal{L}^{-1}} = \sup_{0 \neq x \in \mathbb{H}} \frac{\langle f, x \rangle}{\|x\|_{\mathcal{L}}} = \sup_{\substack{x \in \mathbb{H} \\ \|x\|_{\mathcal{L}}=1}} \langle f, x \rangle, \quad \forall f \in \mathbb{H}'.$$

Finally, we have

$$(2.8) \quad \|\mathcal{L}^{-1}f\|_{\mathcal{L}} = \|f\|_{\mathcal{L}^{-1}}, \quad \forall f \in \mathbb{H}' \quad \text{and} \quad \|\mathcal{L}x\|_{\mathcal{L}^{-1}} = \|x\|_{\mathcal{L}}, \quad \forall x \in \mathbb{H}.$$

Remark 2.3 (no preconditioning). Suppose that $\mathfrak{R}_{\mathbb{H}} : \mathbb{H}' \rightarrow \mathbb{H}$ is the canonical Riesz map, that is, the Riesz map with respect to the canonical inner product $(\cdot, \cdot)_{\mathbb{H}}$. We can set $\mathcal{L} = \mathfrak{R}_{\mathbb{H}}^{-1}$. If we do this, we find that the \mathcal{L} -inner product reduces to the original inner product, $(\cdot, \cdot)_{\mathbb{H}}$: for $x, y \in \mathbb{H}$,

$$(x, y)_{\mathcal{L}} = \langle \mathcal{L}x, y \rangle = (\mathfrak{R}_{\mathbb{H}}\mathcal{L}x, y)_{\mathbb{H}} = (x, y)_{\mathbb{H}}.$$

■

Our objective $G : \mathbb{H} \rightarrow \mathbb{R}$ will be assumed to be Fréchet differentiable at every point in \mathbb{H} . We denote by $G'(x) \in \mathbb{H}'$ the Fréchet derivative of G at the point $x \in \mathbb{H}$. Since the definition of Fréchet differentiability involves a norm, the actual derivative is possibly norm dependent. The following result shows that, actually, the definition is invariant as long as the norms are equivalent.

Proposition 2.4 (equivalent norms). *Let \mathbb{H} be a real and separable Hilbert space with norm $\|\cdot\|_{\mathbb{H}}$, and $G : \mathbb{H} \rightarrow \mathbb{R}$ be Fréchet differentiable at $x \in \mathbb{H}$. Assume that $\|\cdot\|_{\mathbb{H}}$ is another norm on \mathbb{H} . If $\|\cdot\|_{\mathbb{H}}$ is equivalent to $\|\cdot\|_{\mathbb{H}}$, then G is also Fréchet differentiable at x with respect to $\|\cdot\|_{\mathbb{H}}$. Furthermore, the derivatives coincide.*

Notice that nothing is said about continuity in the previous statement. For convex functions, the continuity of the derivatives is automatic once the Fréchet differentiability is guaranteed [18, p. 20 Corollary].

Proposition 2.5 (continuity). *Let \mathbb{H} be a real and separable Hilbert space and $D \subset \mathbb{H}$ be open and convex. If $G : D \rightarrow \mathbb{R}$ is convex and Fréchet differentiable, then $x \mapsto G'(x)$ is norm continuous on D .*

The following two definitions provide a framework to describe the geometry of the graph of our objective functional.

Definition 2.6 (Lipschitz smoothness). Let \mathbb{H} be a real and separable Hilbert space, and $G : \mathbb{H} \rightarrow \mathbb{R}$ be Fréchet differentiable at every point. We say that G is *locally Lipschitz smooth* (with respect to \mathcal{L} -norm) iff, for every bounded, convex set $B \subset \mathbb{H}$, there exists a constant $L_B > 0$ such that

$$(2.9) \quad \langle G'(x) - G'(y), x - y \rangle \leq L_B \|y - x\|_{\mathcal{L}}^2 \quad \forall x, y \in B.$$

For brevity, we say that G is L_B -smooth on B . If the constant $L_B = L > 0$ can be chosen to be independent of B , then we say that G is *globally Lipschitz smooth with a constant L* , or simply L -smooth.

Remark 2.7 (terminology). The above definition is a weaker notion than the local Lipschitz continuity of the Fréchet derivative of G , which is given by

$$(2.10) \quad \|G'(x) - G'(y)\|_{\mathcal{L}^{-1}} \leq L_B \|x - y\|_{\mathcal{L}} \quad \forall x, y \in B,$$

for some $L_B > 0$. Of course, this implies the local Lipschitz smoothness of G (2.9). In this paper, to avoid confusion, whenever (2.10) holds, we will say that G is *locally Lipschitz smooth in the strong sense* or that G' is *locally Lipschitz in the strong sense*. We need this stronger condition when we obtain the existence and uniqueness of the IVP which corresponds to the limiting case of PAGD (Lemma 4.2). Note, however, for convex functions, the global versions of the two definitions are equivalent. That is, if $B = \mathbb{H}$, (2.9) implies (2.10) [17, Theorem 2.1.5 (2.1.8)].

Definition 2.8 (strong convexity). Let $G : \mathbb{H} \rightarrow \mathbb{R}$ be Fréchet differentiable. We say that G is μ -strongly convex (with respect to \mathcal{L} -norm) iff there exists a constant $\mu > 0$ such that

$$(2.11) \quad \langle G'(x) - G'(y), x - y \rangle \geq \mu \|y - x\|_{\mathcal{L}}^2 \quad \forall x, y \in \mathbb{H}.$$

We now state an equivalent characterization of these notions.

Theorem 2.9 (equivalence). Let \mathbb{H} be a real and separable Hilbert space, and $G : \mathbb{H} \rightarrow \mathbb{R}$ be Fréchet differentiable. G is L_B -smooth on the bounded convex set $B \subset \mathbb{H}$ if and only if

$$(2.12) \quad G(y) - G(x) - \langle G'(x), y - x \rangle \leq \frac{L_B}{2} \|y - x\|_{\mathcal{L}}^2 \quad \forall x, y \in B.$$

Similarly, G is μ -strongly convex if and only if

$$(2.13) \quad G(y) - G(x) - \langle G'(x), y - x \rangle \geq \frac{\mu}{2} \|y - x\|_{\mathcal{L}}^2 \quad \forall x, y \in \mathbb{H}.$$

Proof. These results follow from Taylor's Theorem with integral remainder. See also [17, Theorem 2.1.5, Theorem 2.1.9]. \square

Among the two characterizations of Lipschitz smoothness and strong convexity stated above, we will call (2.12) and (2.13) the upper and the lower *quadratic trap* of G , respectively. The constant $\frac{L_B}{\mu}$ is called the *(local) condition number* of the objective functional G with respect to the \mathcal{L} -norm. In what follows, we will use its reciprocal, denoted by $\rho = \frac{\mu}{L_B} \in (0, 1]$, to quantify rates of convergence. Note that the condition number crucially depends on the norm that is used to describe the geometry of the graph of G . Choosing a good preconditioner, \mathcal{L} , is at the heart of much of scientific computing.

We conclude this section by stating a pair of well-known identities which we will use frequently. For any $A, B \in \mathbb{H}$,

$$(2.14) \quad (A, B)_{\mathcal{L}} = \frac{1}{2} \|A\|_{\mathcal{L}}^2 + \frac{1}{2} \|B\|_{\mathcal{L}}^2 - \frac{1}{2} \|A - B\|_{\mathcal{L}}^2$$

$$(2.15) \quad = \frac{1}{2} \|A + B\|_{\mathcal{L}}^2 - \frac{1}{2} \|A\|_{\mathcal{L}}^2 - \frac{1}{2} \|B\|_{\mathcal{L}}^2.$$

3. OPTIMIZATION SCHEMES

To put our contributions in context, here we briefly review several algorithms that are closely related to our main algorithm of interest, the preconditioned Nesterov's accelerated gradient descent methods (PAGD). To focus on the main differences between the schemes of interest, we will not pay attention to choices of step size and stopping criteria of the algorithms. For those readers who are interested in these details, we refer, for instance, to [17, 6, 4, 9].

Algorithm 1: Preconditioned gradient descent method (PGD)

Data: G : The objective
Data: $s > 0$: The step size
Data: $x_0 \in \mathbb{H}$: The initial guess
Result: The sequence $\{x_k\}_{k \geq 1}$ that approximates x^* , the minimizer of G
for $k \geq 0$ **do**
 $x_{k+1} = x_k - s\mathcal{L}^{-1}G'(x_k);$
end

We begin by presenting the PGD scheme in Algorithm 1 and describing its convergence properties. To do so, we introduce

$$B = \{x \in \mathbb{H} \mid G(x) \leq G(x_0)\},$$

which is a bounded, convex set containing the minimizer. Then, assuming that G is L_B -smooth on B and μ -strongly convex, and that the step size satisfies $s \in (0, 2/(L_B + \mu)]$, it is possible to show that $x_k \in B$ for all $k \geq 0$. Moreover, in this setting, the scheme converges exponentially fast to the minimizer [13, 9, 17]. In particular, if $s = 2/(L_B + \mu)$, then

$$(3.1) \quad \|x_k - x^*\|_{\mathcal{L}} \leq \left(\frac{1-\rho}{1+\rho}\right)^k \|x_0 - x^*\|_{\mathcal{L}}.$$

Algorithm 2: Preconditioned accelerated gradient descent method (PAGD)

Data: G : The objective
Data: $\mu > 0$: The strong convexity constant of G
Data: $s > 0$: The step size
Data: $x_0 \in \mathbb{H}$: The initial guess
Result: The sequence $\{x_k\}_{k \geq 1}$ that approximates x^* , the minimizer of G
Define: $\theta = \sqrt{s\mu}$ **and** $\lambda = \frac{1-\theta}{1+\theta};$
Set: $y_0 = v_0 = x_0 \in \mathbb{H};$
for $k \geq 0$ **do**
 (3.2) $x_{k+1} = y_k - s\mathcal{L}^{-1}G'(y_k),$
 (3.3) $y_{k+1} = x_{k+1} + \lambda(x_{k+1} - x_k),$
 (3.4) $v_{k+1} = x_k + \frac{1}{\theta}(x_{k+1} - x_k).$
end

To improve on the convergence of GD (Algorithm 1 with $\mathcal{L} = \mathfrak{R}_{\mathbb{H}}^{-1}$) Nesterov, in [16], devised an algorithm, which “accelerates” the rate of convergence of GD. The improved algorithm is commonly known as *Nesterov’s accelerated gradient descent method* (AGD). The preconditioned version of this scheme, PAGD, is presented in Algorithm 2. As we will see in Section 5, for convergence, the algorithm must satisfy the condition $s \leq 1/L_B$, where $L_B > 0$ is the (local) Lipschitz smoothness constant of G with respect to a bounded convex neighborhood, B , of the minimizer. Notice that an actual implementation does not need to compute the sequence $\{v_k\}_{k \geq 0}$.

It must be noted that PAGD, as presented in Algorithm 2, is practical only if the objective functional is μ -strongly convex ($\mu > 0$). Otherwise, a convergence result may not be available. There exists a more general scheme, which one may call *accelerated gradient descent method with variable weights* [17, p. 78], that is applicable to merely convex objectives. We do not discuss this case here.

Let us now compare the existing performance of GD and AGD (Algorithm 1 and Algorithm 2 with $\mathcal{L} = \mathfrak{R}_{\mathbb{H}}^{-1}$ respectively) by comparing $G(x_k) - G^*$, where k is the number of iterations and $G^* = G(x^*)$ is the minimum of G . To the best of our knowledge, the existing results on AGD are established under the assumption that the objective is *globally* Lipschitz smooth. Thus, for the rest of the summary of this section, the objective G is assumed to be (globally) L -smooth. If GD is applied to a (merely) convex, L -smooth objective functional with a step size condition $0 < s \leq 1/L$, then we have a first order convergence in the objective functional, i.e., $G(x_k) - G^* \leq O(1/k)$ as $k \rightarrow \infty$ [17, Corollary 2.1.2]. On the other hand, AGD with variable weights (the more general version mentioned above) provides a second order convergence, that is, $G(x_k) - G^* \leq O(1/k^2)$ as $k \rightarrow \infty$. If the objective is, in addition, μ -strongly convex, the convergence rates of the two schemes become exponential. Specifically, estimate (3.1) and the quadratic traps show that the convergence rate of GD is $G(x_k) - G^* \leq O((\frac{1-\rho}{1+\rho})^{2k})$ as $k \rightarrow \infty$, where we recall that $\rho = \mu/L$. This is in contrast to AGD, which converges with a rate of $G(x_k) - G^* \leq O((1 - \sqrt{\rho})^k)$ as $k \rightarrow \infty$; see [17, Theorem 2.2.3]. If $\rho \ll 1$, this acceleration can be significant. The contraction factors are $(\frac{1-\rho}{1+\rho})^2$ and $(1 - \sqrt{\rho})$ respectively. Thus, for example, if $\rho \leq 1/16$, hence $4\sqrt{\rho} \leq 1$, then

$$\left(\frac{1-\rho}{1+\rho}\right)^2 = \left(1 - 2\rho \frac{1}{1+\rho}\right)^2 \geq (1 - 2\rho)^2 = 1 - 4\rho + 4\rho^2 \geq 1 - 4\rho \geq 1 - \sqrt{\rho}.$$

As we will see later, PAGD achieves the same rate of exponential convergence even if the objective is locally Lipschitz smooth instead of the Lipschitz smoothness being imposed globally.

4. AN ODE MODEL FOR PAGD

Despite the significant improvement in convergence rate that PAGD exhibits, it is hard to intuitively see how the acceleration is achieved. Many have sought to provide such an explanation; see [21, 22, 2]. In this section, we build on the results of [21] and look at an ODE that models the behavior of the PAGD scheme.

Reference [21] derives a second order ODE whose solution is the limiting trajectory (as step size approaches 0) of a variant of AGD to minimize a merely convex, L -smooth objective G . This reference also shows the second order decay in time of the objective functional along the trajectory. That is, $G(X(t)) - G^* \leq O(1/t^2)$ as $t \rightarrow \infty$, where $X : [0, \infty) \rightarrow \mathbb{H}$ is the solution of the ODE with appropriate initial

conditions associated with the scheme. This corresponds to Nesterov’s second order (discrete) acceleration that is mentioned in the introduction and proved in [16].

We will conduct a similar analysis in the locally Lipschitz smooth, strongly convex setting. We must point out, however, that we analyze a different scheme from the one that is studied in [21]. We analyze Algorithm 2, whose associated ODE exhibits an (accelerated) exponential rate of decay of the objective functional along the solution whereas the scheme that they analyzed shows a polynomial decay in time even with a strongly convex objective. Likewise, Wibisono et al. [22] mainly analyzed a *polynomial Lagrangian flow* as a limiting case of AGD, which also exhibits only polynomial convergence rate even with strongly convex objective functionals. They did show an exponential convergence of a variant of AGD, what they call an accelerated method with restart scheme, but they did not analyze the link to continuous time.

To streamline the discussion, we start by directly introducing the initial value problem (IVP) whose certain discretization leads to PAGD:

$$(4.1) \quad \begin{cases} \ddot{X}(t) + 2\eta\dot{X}(t) + \mathcal{L}^{-1}G'(X(t)) = 0, & t > 0, \\ X(0) = x_0, \\ \dot{X}(0) = 0. \end{cases}$$

See Appendix A for its derivation. A specific discretization, which will eventually lead to Algorithm 2, is introduced after analyzing and discussing the convergence to equilibrium of the IVP (4.1); see Section 4.2. This is deferred because we need to introduce more ingredients and physical intuition.

Remark 4.1 (physical interpretation). This IVP (4.1) describes the motion of a particle of unit mass in the potential G with friction coefficient 2η which starts from the initial position x_0 at rest. For example, we can think of a rolling ball on a sticky bowl released at some initial position. Thus, our physical intuition suggests that the particle will converge to its minimal point as, under the action of friction, it exhausts the initial “total energy,” i.e., the sum of its potential and kinetic energies. If the friction, quantified by η , is too small it will oscillate as it reaches the minimal point and it will converge only after a long travel. On the other hand, if the friction is too large, it will not move sufficiently rapidly, and this, in turn, will also lead to slow convergence. Let us compare this with another physical system. We can interpret the physics of the gradient flow as a limiting case of the same dynamics. The gradient flow

$$\dot{X}(t) = -\mathcal{L}^{-1}G'(X(t))$$

can be viewed, up to a constant factor 2η , as a massless limit of the IVP (4.1). That is, a physical thought experiment suggests that the surroundings hold the particle back as soon as it gets accelerated since it is so light. A real life example of this kind is a very viscous fluid, such as honey, flowing down a bowl. Our physical experience suggests that it will not oscillate and will flow along the steepest descent direction every moment. However, it will reach the bottom slower than the rolling ball will if the friction is appropriately strong. ■

4.1. Analysis of the IVP. As one can expect from the fact that the IVP (4.1) describes a concrete physical situation, its solution possesses good properties. In this and the following section, however, we need a slightly stronger assumption on G than in the rest of the discussion.

Lemma 4.2 (existence and uniqueness). *Suppose that $G : \mathbb{H} \rightarrow \mathbb{R}$ is μ -strongly convex and locally Lipschitz smooth in the strong sense, i.e., (2.10) holds. Then, for any $T > 0$, there exists a unique solution $X \in C^2(0, T; \mathbb{H})$ to the initial value problem (4.1) and the solution obeys the following energy identity*

$$(4.2) \quad \frac{1}{2} \|\dot{X}(t)\|_{\mathcal{L}}^2 + G(X(t)) - G^* = G(x_0) - G^* - 2\eta \int_0^t \|\dot{X}(\tau)\|_{\mathcal{L}}^2 d\tau \quad \forall t \geq 0.$$

Consequently, the solution exists for all $t \in [0, \infty)$ and it is twice continuously differentiable.

Proof. By introducing an auxiliary variable $W : [0, \infty) \rightarrow \mathbb{H}$, the IVP (4.1) can be equivalently written as a system of first order ODEs

$$(4.3) \quad \begin{cases} \dot{X}(t) = W(t), & t > 0, \\ \dot{W}(t) = -2\eta W(t) - \mathcal{L}^{-1}G'(X(t)), & t > 0, \\ X(0) = x_0, \\ W(0) = 0. \end{cases}$$

System (4.3) can be written as

$$\dot{Z}(t) = F(t, Z), \quad t > 0, \quad Z(0) = (x_0, 0),$$

where $Z = (X, W) : [0, \infty) \rightarrow \mathbb{H}^2$ and $F : (0, \infty) \times \mathbb{H}^2 \rightarrow \mathbb{H}^2$ is defined via

$$F(t, Z) = (W, -2\eta W - \mathcal{L}^{-1}G'(X)).$$

It is immediate to see that F is continuous and locally Lipschitz in the strong sense in the second argument. Thus, owing to the Picard-Lindelöf theorem on Banach spaces [8, p. 110 Theorem 1.8.1], we have local existence and uniqueness of a classical solution, say on $[0, T)$ for some $T > 0$. In particular, $W = \dot{X} \in C^1(0, T; \mathbb{H})$ implies that $X \in C^2(0, T; \mathbb{H})$. Moreover, this classical solution must coincide with the mild solution represented by

$$(4.4) \quad Z(t) = (x_0, 0) + \int_0^t F(\tau, Z(\tau)) d\tau, \quad t \in [0, T).$$

We now show the energy law (4.2), which will lead to the global existence of the solution. Let us take the \mathcal{L} -inner product of the first equation of (4.1) with \dot{X} and integrate over time $\tau \in [0, t]$. We obtain

$$\int_0^t (\ddot{X}(\tau), \dot{X}(\tau))_{\mathcal{L}} d\tau + 2\eta \int_0^t \|\dot{X}(\tau)\|_{\mathcal{L}}^2 d\tau + \int_0^t \langle G'(X(\tau)), \dot{X}(\tau) \rangle d\tau = 0.$$

Noting that $(\ddot{X}(t), \dot{X}(t))_{\mathcal{L}} = \frac{1}{2} \frac{d}{dt} \|\dot{X}(t)\|_{\mathcal{L}}^2$ and $\langle G'(X(t)), \dot{X}(t) \rangle = \frac{d}{dt} G(X(t))$, rearranging, and subtracting the minimum G^* from both sides, we obtain the energy identity (4.2) upon plugging in the initial conditions.

By discarding the velocity term and the integral term from (4.2), we obtain an upper bound on the distance between $X(t)$ and the minimizer x^* . That is, in conjunction with the strong convexity of G , we have $\frac{\mu}{2} \|X(t) - x^*\|_{\mathcal{L}}^2 \leq G(X(t)) - G^* \leq G(x_0) - G^*$, which, in turn, provides

$$(4.5) \quad \|X(t) - x^*\|_{\mathcal{L}} \leq \sqrt{\frac{2}{\mu} (G(x_0) - G^*)}.$$

Similarly, by removing different terms from (4.2), it follows that $\frac{1}{2}\|\dot{X}(t)\|_{\mathcal{L}}^2 \leq G(x_0) - G^*$, from which we obtain

$$(4.6) \quad \|\dot{X}(t)\|_{\mathcal{L}} = \|W(t)\|_{\mathcal{L}} \leq \sqrt{2(G(x_0) - G^*)}.$$

Estimates (4.5) and (4.6) ensure that the integrand involved in the definition of the mild solution (4.4) is uniformly bounded in t , hence $\lim_{t \uparrow T}(X(t), W(t))$ exists. Therefore, the local solution continues to exist for $[0, T + \varepsilon)$ for some $\varepsilon > 0$; see [8, p. 111]. The global existence of the solution follows by repeating this argument. \square

Remark 4.3 (smoothness of the solution). The fact that

$$X \in C^2((0, \infty); \mathbb{H}) \cap C([0, \infty); \mathbb{H})$$

justifies the manipulations we will carry out when we derive the IVP (4.1) in Appendix A. \blacksquare

4.2. Convergence to equilibrium. We now wish to prove that the solution to the IVP (4.1) with G being locally Lipschitz smooth and μ -strongly convex converges to its attractive steady state solution as $t \rightarrow \infty$, which is the minimal point in this case, at a matching rate with that of PAGD. This is one of the highlights of this work. To this end, we introduce an auxiliary variable

$$V(t) = X(t) - x^* + \frac{1}{\eta} \dot{X}(t)$$

so that the first equation of the IVP (4.1) can be rewritten

$$(4.7) \quad \eta \dot{V}(t) + \eta \dot{X}(t) + \mathcal{L}^{-1} G'(X(t)) = 0.$$

We also introduce an energy

$$(4.8) \quad E(X, V) = \frac{\eta}{2} \|V\|_{\mathcal{L}}^2 + \frac{1}{\eta} (G(X) - G^*),$$

where we recall $G^* = G(x^*) = \min_{x \in \mathbb{H}} G(x)$. We will show that E is a *Lyapunov* function for the IVP (4.1). For notational convenience, set

$$(4.9) \quad E_0 = E(x_0, x_0) = \frac{1}{\eta} (G(x_0) - G^*) + \frac{\eta}{2} \|x_0 - x^*\|_{\mathcal{L}}^2.$$

Theorem 4.4 (exponential decay). *Let $G : \mathbb{H} \rightarrow \mathbb{R}$ be locally Lipschitz smooth in the strong sense and μ -strongly convex. Denote by X the unique solution to the IVP (4.1). If $\eta^2 \leq \mu$, the exponentially inflated energy $\mathcal{E}(t) = e^{\eta t} E(X(t), V(t))$ is nonincreasing. Consequently, the Lyapunov function (4.8) decays to zero at an exponential rate:*

$$E(X(t), V(t)) = \frac{\eta}{2} \|V(t)\|_{\mathcal{L}}^2 + \frac{1}{\eta} (G(X(t)) - G^*) \leq e^{-\eta t} E_0.$$

Proof. Existence and uniqueness of X is guaranteed by Lemma 4.2. Let us now prove the estimate on the energy E . Taking the inner product of (4.7) with $V(t)$,

and using the identity (2.14), we obtain, suppressing the time variable,

$$\begin{aligned}
(4.10) \quad 0 &= \eta(V, \dot{V})_{\mathcal{L}} + \eta(\dot{X}, X - x^* + \frac{1}{\eta}\dot{X})_{\mathcal{L}} + (\mathcal{L}^{-1}G'(X), X - x^*)_{\mathcal{L}} \\
&\quad + \frac{1}{\eta}(\mathcal{L}^{-1}G'(X), \dot{X})_{\mathcal{L}} \\
&= \eta(V, \dot{V})_{\mathcal{L}} + \frac{1}{2}\|\dot{X}\|_{\mathcal{L}}^2 + \frac{\eta^2}{2}\|V\|_{\mathcal{L}}^2 - \frac{\eta^2}{2}\|X - x^*\|_{\mathcal{L}}^2 + \langle G'(X), X - x^* \rangle \\
&\quad + \frac{1}{\eta}\langle G'(X), \dot{X} \rangle.
\end{aligned}$$

The lower quadratic trap, (2.13), implies

$$(4.11) \quad G(X) - G^* - \langle G'(X), X - x^* \rangle \leq -\frac{\mu}{2}\|X - x^*\|_{\mathcal{L}}^2.$$

Substituting (4.10) into the time derivative of the inflated energy and then using the above estimate (4.11), we have

$$\begin{aligned}
(4.12) \quad \dot{\mathcal{E}}(t) &= e^{\eta t} \left[\frac{\eta^2}{2}\|V\|_{\mathcal{L}}^2 + \eta(V, \dot{V})_{\mathcal{L}} + (G(X) - G^*) + \frac{1}{\eta}\langle G'(X), \dot{X} \rangle \right] \\
&= e^{\eta t} \left[-\frac{1}{2}\|\dot{X}\|_{\mathcal{L}}^2 + \frac{\eta^2}{2}\|X - x^*\|_{\mathcal{L}}^2 - \langle G'(X), X - x^* \rangle + G(X) - G^* \right] \\
&\leq -\frac{1}{2}e^{\eta t} \left[\|\dot{X}\|_{\mathcal{L}}^2 + \frac{\mu - \eta^2}{2}\|X - x^*\|_{\mathcal{L}}^2 \right].
\end{aligned}$$

The last term is always nonpositive provided $\eta^2 \leq \mu$, and this implies $\mathcal{E}(t) \leq \mathcal{E}(0) = E_0$. This completes the proof. \square

Remark 4.5 (convergence of the objective). Since the parameter λ of PAGD scheme leads to $\eta = \sqrt{\mu}$, the solution to the corresponding IVP (4.1) satisfies the following exponential decay of the objective functional:

$$(4.13) \quad G(X(t)) - G^* \leq e^{-\eta t} E_0. \quad \blacksquare$$

Remark 4.6 (physical interpretation). We can rigorously explain the physical intuition given in Remark 4.1 through Theorem 4.4 and its proof. If the friction, quantified by η , is too small the decay to the attraction point is slow as η governs the decay rate $e^{-\eta t}$. On the other hand, If the friction is too large, say $\eta > \sqrt{\mu}$, then we cannot guarantee the boundedness of $\mathcal{E}(t)$. \blacksquare

4.3. PAGD as a discretization of the IVP. PAGD can be viewed as a discretization of an ODE although not every choice in the process can be seen as natural or intuitive.

Let us label the step size \sqrt{s} , rather than calling it s , in order to make the setting more in line with the actual PAGD algorithm. The main iterates that represent the position of a particle are identified via $x_k = X(k\sqrt{s})$ (see Remark 4.1 for the physical interpretation). In addition to that, we want to introduce certain extrapolations to approximate $X((k+1)\sqrt{s})$. By removing potential terms from the first equation of (4.1), we can model how the particle moves on a small time interval $[t, t + \sqrt{s}]$ with no effect of the potential energy landscape, i.e., we are interested

in what the future position would be if there were only the effect of inertia and frictions for a short period of time:

$$\ddot{X}(t) + 2\eta\dot{X}(t) = 0.$$

Taking the \mathcal{L} -inner product of this with $\dot{X}(t)$ and integrating over $[t, t + \sqrt{s}]$, we get

$$\frac{1}{2}\|\dot{X}(t + \sqrt{s})\|_{\mathcal{L}}^2 = \frac{1}{2}\|\dot{X}(t)\|_{\mathcal{L}}^2 - 2\eta \int_t^{t+\sqrt{s}} \|\dot{X}(\tau)\|_{\mathcal{L}}^2 d\tau.$$

We approximate the speed in the integrand by the average of those at the end points $\frac{1}{2}(\|\dot{X}(t + \sqrt{s})\|_{\mathcal{L}} + \|\dot{X}(t)\|_{\mathcal{L}})$, rearrange terms, and set $\theta = \sqrt{\mu s} = \eta\sqrt{s}$ to obtain

$$(1 + \theta)\|\dot{X}(t + \sqrt{s})\|_{\mathcal{L}}^2 + 2\theta\|\dot{X}(t + \sqrt{s})\|_{\mathcal{L}}\|\dot{X}(t)\|_{\mathcal{L}} - (1 - \theta)\|\dot{X}(t)\|_{\mathcal{L}}^2 = 0,$$

which factors and results in $\|\dot{X}(t + \sqrt{s})\|_{\mathcal{L}} = \lambda\|\dot{X}(t)\|_{\mathcal{L}}$, where we assume $\|\dot{X}(t + \sqrt{s})\|_{\mathcal{L}}, \|\dot{X}(t)\|_{\mathcal{L}} \neq 0$ and recall $\lambda = \frac{1-\theta}{1+\theta}$. Since our dynamics is taking place in the same direction on a straight line, there is no problem with getting an equality for vectors from this equality in norms:

$$\dot{X}(t + \sqrt{s}) = \lambda\dot{X}(t).$$

Also, we approximate $\dot{X}(t)$ by backward difference with $X(t) = x_k$ and $X(t - \sqrt{s}) = x_{k-1}$, and $\dot{X}(t + \sqrt{s})$ with $X(t) = x_k$ and the extrapolation $X(t + \sqrt{s}) \approx y_k$ to obtain

$$y_k - x_k = \lambda(x_k - x_{k-1}),$$

which is the definition of $\{y_k\}_{k \geq 1}$. Note that we reserve the iterate x_{k+1} for the approximation of $X(t + \sqrt{s})$ with the effect of the potential energy included.

Next, we discretize the vector $V(t)$. Since we do not know the minimizer in practice, we remove it from the definition of v_k . That is, we discretize $V(t) + x^* = X(t) + \frac{1}{\eta}\dot{X}(t)$ to define v_k . We use the extrapolation for $X(t)$ and the forward difference with extrapolation for $\dot{X}(t)$ so that $X(t) \approx y_k$ and $\dot{X}(t) \approx (y_k - x_k)/\sqrt{s}$ respectively, which suggests

$$(4.14) \quad v_k = y_k + \frac{1}{\theta}(y_k - x_k).$$

This leads to the definition of $\{v_k\}_{k \geq 1}$ (3.4) upon combining with the definition of $\{y_k\}_{k \geq 1}$.

Finally, to get the main iterates, $\{x_k\}_{k \geq 1}$, we discretize (4.7) using the usual forward difference for $\dot{V}(t)$, the forward difference with extrapolation for $\dot{X}(t)$ as before, and the evaluation of G' at the extrapolated point, then it follows

$$\eta \frac{v_{k+1} - v_k}{\sqrt{s}} + \eta \frac{y_k - x_k}{\sqrt{s}} + \mathcal{L}^{-1}G'(y_k) = 0.$$

Multiplying this by s , plugging in the definition of v_{k+1} (3.4) and (4.14), one obtains (3.2), the definition of $\{x_k\}_{k \geq 1}$. Hence, we have obtained the PAGD scheme as a, somewhat nonstandard, discretization of (4.1).

Remark 4.7 (momentum method). A similar procedure can be carried out far more easily for the so-called *momentum method* (MM). To see this, we recall that

$$\ddot{X}(t) \approx \frac{x_{k+1} - 2x_k + x_{k-1}}{s}, \quad \dot{X}(t) \approx \frac{x_k - x_{k-1}}{\sqrt{s}}, \quad G'(X(t)) \approx G'(x_k).$$

Then, the discrete version of the ODE (4.1) becomes

$$x_{k+1} = x_k - sG'(x_k) + (1 - 2\eta\sqrt{s})(x_k - x_{k-1}),$$

which is MM with the weight $1 - 2\eta\sqrt{s}$; see [19, p. 12 (9)]. This weight is close to λ :

$$\lambda = \frac{1 - \eta\sqrt{s}}{1 + \eta\sqrt{s}} = 1 - \frac{2\eta\sqrt{s}}{1 + \eta\sqrt{s}} \approx 1 - 2\eta\sqrt{s}.$$

In this sense, MM seems more natural and amenable for analysis than AGD. \blacksquare

The limiting behavior of MM can also be explained by the IVP (4.1). Observe that the only essential difference between MM and PAGD is where G' is evaluated, that is, x_k and y_k respectively. And in the limit $s \rightarrow 0$, x_k and y_k are not distinguishable. However, PAGD exhibits less oscillation than MM since evaluating G' at y_k serves as “foreseeing” the uphill of the objective functional, if exists, along the trajectory and “steering” to avoid unnecessary oscillating behaviors.

5. AN ENERGY APPROACH TO CONVERGENCE OF PAGD

In this section, we derive an exponential rate of convergence for PAGD in the case of strongly convex, locally Lipschitz smooth objectives, which follows the ODE arguments developed in Section 4. Although this result is already known; see, for instance, [17], the existing proofs have puzzled many people. The proof that is presented here, on the other hand, reveals a rich structure of the scheme as it mimics the ODE approach that we discussed in Section 4.

As a first step, we show that the assumption of the local Lipschitz smoothness is sufficient for our analysis, as the iterates lie within a bounded set. We first show that, for every $k \geq 0$, the y_k iterate of PAGD lies in the segment between x_k and v_k . This is used frequently in the convergence proof.

Lemma 5.1 (convex hull). *For every $k \geq 0$, the iterates constructed in PAGD, described in Algorithm 2, satisfy $y_k \in \overline{x_k v_k}$. Specifically, they satisfy the following four equivalent equations:*

$$(5.1) \quad \begin{cases} y_k = \frac{1}{1+\theta}x_k + \frac{\theta}{1+\theta}v_k, & x_k = (1+\theta)y_k - \theta v_k, \\ v_k = \left(1 + \frac{1}{\theta}\right)y_k - \frac{1}{\theta}x_k, & x_k - y_k = \theta(y_k - v_k). \end{cases}$$

Proof. If $k = 0$ this is trivial since $x_0 = y_0 = v_0$. For $k \geq 1$, we eliminate x_{k-1} from (3.3) and (3.4) with the index being $k - 1$ to get

$$\left(1 - \frac{1}{\theta}\right)y_k + \lambda v_k = \left((1+\lambda)\left(1 - \frac{1}{\theta}\right) + \frac{\lambda}{\theta}\right)x_k = -\frac{\lambda}{\theta}x_k.$$

Rearranging terms and using $\lambda = \frac{1-\theta}{1+\theta}$, we obtain the equalities that are listed above. \square

We now show that there is an invariant set for the iterates of PAGD.

Lemma 5.2 (invariant set). *Assume that the objective $G : \mathbb{H} \rightarrow \mathbb{R}$ is μ -strongly convex and locally Lipschitz smooth. Define*

$$(5.2) \quad B = \{x \in \mathbb{H} \mid \|x - x^*\|_{\mathcal{L}} \leq R\},$$

where $R = R_1 + \frac{1}{\eta}R_2$, $R_1 = \sqrt{\frac{2}{\mu}(G(x_0) - G^*)}$, $R_2 = \sqrt{2r(G(x_0) - G^*)}$, and $r > 1$. Let PAGD, as described in Algorithm 2, be implemented with a step size rule

$$(5.3) \quad s \in \left(0, \min \left\{ L_B^{-1}, \left(\frac{r-1}{r+1} \right)^2 \mu^{-1} \right\} \right],$$

where L_B the local Lipschitz smoothness constant of G associated to the set B . Then, for all $k \geq 0$, we have that $\|x_k - x^*\|_{\mathcal{L}} \leq R_1$, hence $x_k \in B$, and $y_k, v_k \in B$.

Proof. The outline of this proof is simple although it is long. We mimic the energy argument developed in Section 4.1 to obtain a bound on the distance between the main iterates and the minimizer and that on the speed. Once we get the bounds, it is easy to prescribe an appropriate ball, which will be our invariant set.

We will prove the statement by induction. For $k = 0$, the statement is trivial since $x_0 = y_0 = v_0$ and the strong convexity implies $\|x_0 - x^*\|_{\mathcal{L}} \leq R_1$. Suppose that $\|x_k - x^*\|_{\mathcal{L}} \leq R_1$ (hence $x_k \in B$) and $y_k, v_k \in B$ are true for $k = 0, 1, 2, \dots, N$. We need to show that $\|x_{N+1} - x^*\|_{\mathcal{L}} \leq R_1$ (hence $x_{N+1} \in B$) and $v_{N+1} \in B$, then Lemma 5.1 implies $y_{N+1} \in \overline{x_{N+1}v_{N+1}} \subset B$ since B is a convex set as a sublevel set of a convex function.

Note that the condition $s \leq \left(\frac{r-1}{r+1}\right)^2 \mu^{-1}$, which is implied by (5.3), ensures λ^{-1} to be bounded above since

$$(5.4) \quad \frac{1}{\lambda} = \frac{1 + \sqrt{s\mu}}{1 - \sqrt{s\mu}} \leq r.$$

First, a similar argument to [9, Proposition 4.6] shows that the x_{N+1} update from y_N is a descent step in terms of G . That is, the section of G across the line $\overleftrightarrow{y_N x_{N+1}}$ also inherits the strong convexity and the local Lipschitz smoothness with the same constants on the one-dimensional affine subset

$$B_{N+1} = \{x = y_N - \tau \mathcal{L}^{-1} G'(y_N) \in \mathbb{H} \mid \tau \in \mathbb{R}\}.$$

Let $S(\tau) = G(y_N - \tau \mathcal{L}^{-1} G'(y_N))$ denote the section.

Since we know that $y_N \in B$, we can bound S in a neighborhood of $\tau = 0$ using the upper quadratic trap

$$\begin{aligned} U(\tau) &:= G(y_N) + \langle G'(y_N), -\tau \mathcal{L}^{-1} G'(y_N) \rangle + \frac{L_B}{2} \|\tau \mathcal{L}^{-1} G'(y_N)\|_{\mathcal{L}}^2 \\ &= G(y_N) - \tau \|G'(y_N)\|_{\mathcal{L}^{-1}}^2 + \frac{L_B \tau^2}{2} \|G'(y_N)\|_{\mathcal{L}^{-1}}^2. \end{aligned}$$

Observe that $S(0) = U(0) = G(y_N)$, that $U(\tau)$ is decreasing around $\tau = 0$ since $dU/d\tau(0) = -\|G'(y_N)\|_{\mathcal{L}^{-1}}^2 \leq 0$, and that the optimal step size to minimize U is $1/L_B$ since $dU/d\tau(1/L_B) = 0$. This implies that $S(s) \leq U(s) \leq U(0)$ for any $s \in [0, 1/L_B]$. Moreover, for $s \in [0, 1/L_B]$, we have

$$(5.5) \quad \begin{aligned} G(x_{N+1}) &= S(s) \leq U(s) = G(y_N) - s \|G'(y_N)\|_{\mathcal{L}^{-1}}^2 + \frac{L_B s^2}{2} \|G'(y_N)\|_{\mathcal{L}^{-1}}^2 \\ &\leq G(y_N) - \frac{s}{2} \|G'(y_N)\|_{\mathcal{L}^{-1}}^2, \end{aligned}$$

which is the desired descent property in G from y_N to x_{N+1} .

Now, we want to mimic the energy argument that we carried out in Section 4.1. Substitute (3.3) into (3.2), and add and subtract $x_k - x_{k-1}$, to obtain the discrete

counterpart of (4.1)

$$(5.6) \quad x_{k+1} - 2x_k + x_{k-1} + (1 - \lambda)(x_k - x_{k-1}) + s\mathcal{L}^{-1}G'(y_k) = 0.$$

Note that defining $x_{-1} := x_0$ allows us to extend this equality to the case $k = 0$. Take the \mathcal{L} -inner product of this identity with $x_k - x_{k-1}$ and add for $0 \leq k \leq N$. Then, using (2.15), the first term telescopes to simplify

$$\begin{aligned} & \sum_{k=0}^N (x_{k+1} - 2x_k + x_{k-1}, x_k - x_{k-1})_{\mathcal{L}} \\ &= \frac{1}{2} \sum_{k=0}^N \left(\|x_{k+1} - x_k\|_{\mathcal{L}}^2 - \|x_{k+1} - 2x_k + x_{k-1}\|_{\mathcal{L}}^2 - \|x_k - x_{k-1}\|_{\mathcal{L}}^2 \right) \\ &= \frac{1}{2} \|x_{N+1} - x_N\|_{\mathcal{L}}^2 - \frac{1}{2} \sum_{k=0}^N \|x_{k+1} - 2x_k + x_{k-1}\|_{\mathcal{L}}^2. \end{aligned}$$

We leave the second term as it is. For the third term, using (3.3), $G(y_k) - G(x_k) \leq \langle G'(y_k), y_k - x_k \rangle$ from convexity, and (5.5), it follows

$$\begin{aligned} & s \sum_{k=0}^N \langle G'(y_k), x_k - x_{k-1} \rangle = \frac{s}{\lambda} \sum_{k=0}^N \langle G'(y_k), y_k - x_k \rangle \\ (5.7) \quad & \geq \frac{s}{\lambda} \sum_{k=0}^N (G(y_k) - G(x_k)) \geq \frac{s}{\lambda} \sum_{k=0}^N \left(G(x_{k+1}) - G(x_k) + \frac{s}{2} \|G'(y_k)\|_{\mathcal{L}^{-1}}^2 \right) \\ &= \frac{s}{\lambda} G(x_{N+1}) - \frac{s}{\lambda} G(x_0) + \frac{s^2}{2\lambda} \sum_{k=0}^N \|G'(y_k)\|_{\mathcal{L}^{-1}}^2. \end{aligned}$$

Gathering all the three terms together and rearranging, we get

$$\begin{aligned} (5.8) \quad & \frac{1}{2} \|x_{N+1} - x_N\|_{\mathcal{L}}^2 + \frac{s}{\lambda} G(x_{N+1}) \leq \frac{s}{\lambda} G(x_0) + \frac{1}{2} \sum_{k=0}^N \|x_{k+1} - 2x_k + x_{k-1}\|_{\mathcal{L}}^2 \\ & - \frac{s^2}{2\lambda} \sum_{k=0}^N \|G'(y_k)\|_{\mathcal{L}^{-1}}^2 - (1 - \lambda) \sum_{k=0}^N \|x_k - x_{k-1}\|_{\mathcal{L}}^2. \end{aligned}$$

Similarly, take the \mathcal{L} -inner product of (5.6) with $x_{k+1} - x_k$ and sum over $0 \leq k \leq N$. This time, use (2.14) for the first term to get

$$\begin{aligned} & \sum_{k=0}^N (x_{k+1} - 2x_k + x_{k-1}, x_{k+1} - x_k)_{\mathcal{L}} \\ &= \frac{1}{2} \|x_{N+1} - x_N\|_{\mathcal{L}}^2 + \frac{1}{2} \sum_{k=0}^N \|x_{k+1} - 2x_k + x_{k-1}\|_{\mathcal{L}}^2. \end{aligned}$$

For the second term, using Cauchy-Schwarz and Young's inequality, we have

$$\begin{aligned} & (1 - \lambda) \sum_{k=0}^N (x_k - x_{k-1}, x_{k+1} - x_k)_{\mathcal{L}} \\ & \geq -\frac{1 - \lambda}{2} \sum_{k=0}^N \left(\|x_k - x_{k-1}\|_{\mathcal{L}}^2 + \|x_{k+1} - x_k\|_{\mathcal{L}}^2 \right). \end{aligned}$$

For the third term, use (3.2) and argue as in (5.7) to get

$$\begin{aligned}
& s \sum_{k=0}^N \langle G'(y_k), x_{k+1} - x_k \rangle = s \sum_{k=0}^N \langle G'(y_k), y_k - s\mathcal{L}^{-1}G'(y_k) - x_k \rangle \\
& \geq -s^2 \sum_{k=0}^N \|G'(y_k)\|_{\mathcal{L}^{-1}}^2 + s \sum_{k=0}^N \langle G'(y_k), y_k - x_k \rangle \\
& \geq sG(x_{N+1}) - sG(x_0) - \frac{s^2}{2} \sum_{k=0}^N \|G'(y_k)\|_{\mathcal{L}^{-1}}^2.
\end{aligned}$$

Gathering all these estimates we get

$$\begin{aligned}
(5.9) \quad & \frac{1}{2} \|x_{N+1} - x_N\|_{\mathcal{L}}^2 + sG(x_{N+1}) \leq sG(x_0) - \frac{1}{2} \sum_{k=0}^N \|x_{k+1} - 2x_k + x_{k-1}\|_{\mathcal{L}} \\
& + \frac{s^2}{2} \sum_{k=0}^N \|G'(y_k)\|_{\mathcal{L}^{-1}}^2 + \frac{1-\lambda}{2} \sum_{k=0}^N \left(\|x_k - x_{k-1}\|_{\mathcal{L}}^2 + \|x_{k+1} - x_k\|_{\mathcal{L}}^2 \right).
\end{aligned}$$

Add (5.8) and (5.9) and rearrange, then after some cancelations, it follows

$$\begin{aligned}
(5.10) \quad & \frac{1+\lambda}{2} \|x_{N+1} - x_N\|_{\mathcal{L}}^2 + s \left(1 + \frac{1}{\lambda} \right) (G(x_{N+1}) - G^*) \\
& \leq s \left(1 + \frac{1}{\lambda} \right) (G(x_0) - G^*) - \frac{s^2}{2} \left(\frac{1}{\lambda} - 1 \right) \sum_{k=0}^N \|G'(y_k)\|_{\mathcal{L}^{-1}}^2
\end{aligned}$$

$$(5.11) \quad \leq s \left(1 + \frac{1}{\lambda} \right) (G(x_0) - G^*),$$

since $0 < \lambda < 1$. By removing the kinetic term from this estimate, strong convexity leads to

$$G(x_0) - G^* \geq G(x_{N+1}) - G^* \geq \frac{\mu}{2} \|x_{N+1} - x^*\|_{\mathcal{L}}^2,$$

which implies

$$(5.12) \quad \|x_{N+1} - x^*\|_{\mathcal{L}} \leq R_1,$$

which, in turn, proves $x_{N+1} \in B$. Similarly, discarding the potential term, dividing through $\frac{s(1+\lambda)}{2}$, and using (5.4), we obtain

$$\left\| \frac{x_{N+1} - x_N}{\sqrt{s}} \right\|_{\mathcal{L}} \leq \sqrt{\frac{2}{\lambda} (G(x_0) - G^*)} \leq R_2.$$

Then, from the definition of v_{N+1} (3.4),

$$\|v_{N+1} - x^*\|_{\mathcal{L}} \leq \|x_N - x^*\|_{\mathcal{L}} + \frac{1}{\eta} \left\| \frac{x_{N+1} - x_N}{\sqrt{s}} \right\|_{\mathcal{L}} \leq R_1 + \frac{1}{\eta} R_2 = R,$$

which implies $v_{N+1} \in B$. This completes the proof. \square

Remark 5.3 (step size restriction). The additional condition $s \leq \left(\frac{r-1}{r+1}\right)^2 \mu^{-1}$ on the step size is not restrictive at all in practice. For example, if $r = 3$, we require that $s \leq 1/4\mu$. The purpose of this condition is to bound λ^{-1} as explained in the proof. However, λ^{-1} becomes unbounded when $s\mu$ is close to 1. If we set $s = 1/L_B$, $s\mu$ is the (inverse) condition number and the (inverse) condition number being close to 1 makes the problem more amenable because it means that G is almost quadratic.

Moreover, even from a theoretical point of view, as r increases, the invariant set B gets larger, which means L_B^{-1} gets smaller, while $(\frac{r-1}{r+1})^2 \mu^{-1}$ approaches μ^{-1} . Since $L_B^{-1} < \mu^{-1}$ (unless G is perfectly quadratic), the second argument of the minimum in (5.3) eventually becomes of no effect. \blacksquare

Corollary 5.4 (convergence of residuals). *Assume that $G : \mathbb{H} \rightarrow \mathbb{R}$ is μ -strongly convex and locally Lipschitz smooth. Suppose that PAGD, as described in Algorithm 2, is implemented with a step size that obeys condition (5.3), where $r > 1$, B is the invariant set given by (5.2), and L_B is the Lipschitz smoothness constant associated with B . In this setting, the residuals $\{G'(y_k)\}_{k \geq 0}$ converge to zero in the \mathcal{L}^{-1} -norm at least ℓ^2 -fast. In other words,*

$$\sum_{k=0}^{\infty} \|G'(y_k)\|_{\mathcal{L}^{-1}}^2 < \infty.$$

Proof. Moving the summation term of (5.10) to the left hand side and dropping the other nonnegative terms, we have

$$\sum_{k=0}^N \|G'(y_k)\|_{\mathcal{L}^{-1}}^2 \leq \frac{2(1+\lambda)}{s(1-\lambda)} (G(x_0) - G^*).$$

Letting $N \rightarrow \infty$ completes the proof. \square

Of course, this result is far from optimal. An exponential convergence of the residuals in the \mathcal{L}^{-1} -norm will be proved in Corollary 5.9.

We can now begin the proof of convergence *per se*. We begin with an estimate for the discrete time derivative of the potential energy.

Lemma 5.5 (discrete derivative of potential energy). *Let the objective $G : \mathbb{H} \rightarrow \mathbb{R}$ be μ -strongly convex and locally Lipschitz smooth. Suppose that the step size in Algorithm 2 satisfies (5.3), where $r > 1$, B is the invariant set given by (5.2), and L_B is the Lipschitz smoothness constant associated with B . Then, we have that*

$$\frac{1}{\eta} \frac{G(x_{k+1}) - G(x_k)}{\sqrt{s}} \leq -\frac{\sqrt{s}}{2\eta} \|G'(y_k)\|_{\mathcal{L}^{-1}}^2 + \frac{1}{\theta} \langle G'(y_k), y_k - x_k \rangle - \frac{\eta}{2\sqrt{s}} \|x_k - y_k\|_{\mathcal{L}}^2.$$

Proof. Since $sL_B \leq 1$, a calculation similar to (5.5) involving L_B -Lipschitz smoothness on B leads to

$$(5.13) \quad G(x_{k+1}) = G(y_k - s\mathcal{L}^{-1}G'(y_k)) \leq G(y_k) - \frac{s}{2} \|G'(y_k)\|_{\mathcal{L}^{-1}}^2.$$

Using this estimate, the strong convexity of G yields

$$\begin{aligned} G(x_k) &\geq G(y_k) + \langle G'(y_k), x_k - y_k \rangle + \frac{\mu}{2} \|x_k - y_k\|_{\mathcal{L}}^2 \\ &\geq G(x_{k+1}) + \frac{s}{2} \|G'(y_k)\|_{\mathcal{L}^{-1}}^2 + \langle G'(y_k), x_k - y_k \rangle + \frac{\mu}{2} \|x_k - y_k\|_{\mathcal{L}}^2. \end{aligned}$$

Rearranging the last estimate, multiplying through by $1/\theta$, and recalling $\theta = \sqrt{s\mu}$, $\eta = \sqrt{\mu}$, we obtain the desired result. \square

We also need an analogue of (4.10), a certain relation derived from the scheme.

Lemma 5.6 (discrete analogue of (4.10)). *The iterates constructed by PAGD, as described in Algorithm 2, satisfy*

$$(5.14) \quad \frac{\eta}{2\sqrt{s}} \left(\|v_{k+1} - x^*\|_{\mathcal{L}}^2 - \|v_k - x^*\|_{\mathcal{L}}^2 \right) + \frac{1}{\theta} \langle G'(y_k), y_k - x_k \rangle + \frac{\eta^2}{2} \|v_k - x^*\|_{\mathcal{L}}^2 \\ - \frac{\eta}{2\sqrt{s}} \|v_{k+1} - v_k\|_{\mathcal{L}}^2 + \frac{1}{2s} \|y_k - x_k\|_{\mathcal{L}}^2 - \frac{\eta^2}{2} \|y_k - x^*\|_{\mathcal{L}}^2 + \langle G'(y_k), y_k - x^* \rangle = 0.$$

Proof. Substituting (3.2) in (3.4), and using the relations (5.1), we have

$$v_{k+1} = x_k + \frac{1}{\theta} (y_k - x_k) - \frac{\sqrt{s}}{\eta} \mathcal{L}^{-1} G'(y_k) = x_k + v_k - y_k - \frac{\sqrt{s}}{\eta} \mathcal{L}^{-1} G'(y_k).$$

Rearranging, and multiplying through by $\frac{\eta}{\sqrt{s}}$, we obtain the discrete analogue of the ODE (4.7)

$$(5.15) \quad \eta \frac{v_{k+1} - v_k}{\sqrt{s}} + \eta \frac{y_k - x_k}{\sqrt{s}} + \mathcal{L}^{-1} G'(y_k) = 0.$$

The discrete analogue of $V(t)$ is $v_k - x^*$, so following the proof of Theorem 4.4, we now take the \mathcal{L} -inner product of (5.15) with $v_k - x^*$ to obtain

$$(5.16) \quad \frac{\eta}{\sqrt{s}} (v_{k+1} - v_k, v_k - x^*)_{\mathcal{L}} + \frac{\eta}{\sqrt{s}} (y_k - x_k, v_k - x^*)_{\mathcal{L}} + \langle G'(y_k), v_k - x^* \rangle = 0.$$

Using (2.15), the first term can be rewritten as

$$\frac{\eta}{\sqrt{s}} (v_{k+1} - v_k, v_k - x^*)_{\mathcal{L}} = \frac{\eta}{2\sqrt{s}} \left(\|v_{k+1} - x^*\|_{\mathcal{L}}^2 - \|v_k - x^*\|_{\mathcal{L}}^2 \right) - \frac{\eta}{2\sqrt{s}} \|v_{k+1} - v_k\|_{\mathcal{L}}^2.$$

For the second term in (5.16), we use relations (5.1), and then the identity (2.14) to get

$$\begin{aligned} \frac{\eta}{\sqrt{s}} (y_k - x_k, v_k - x^*)_{\mathcal{L}} &= \frac{\eta}{\sqrt{s}} \frac{1}{\theta} (y_k - x_k, \theta v_k - \theta x^*)_{\mathcal{L}} \\ &= \frac{1}{s} (y_k - x_k, y_k - x_k + \theta(y_k - x^*))_{\mathcal{L}} \\ &= \frac{1}{2s} \|y_k - x_k\|_{\mathcal{L}}^2 + \frac{\eta^2}{2} \|v_k - x^*\|_{\mathcal{L}}^2 - \frac{\eta^2}{2} \|y_k - x^*\|_{\mathcal{L}}^2. \end{aligned}$$

Finally, for the third term of (5.16), we use (5.1) similarly to the above, then it follows

$$\begin{aligned} \langle G'(y_k), v_k - x^* \rangle &= \frac{1}{\theta} \langle G'(y_k), \theta v_k - \theta x^* \rangle \\ &= \frac{1}{\theta} \langle G'(y_k), y_k - x_k \rangle + \langle G'(y_k), y_k - x^* \rangle. \end{aligned}$$

Then, the desired result follows upon combining the last three identities. \square

We need one more relation between the iterates.

Lemma 5.7 (relation between iterates). *The iterates constructed by PAGD, as described in Algorithm 2, satisfy*

$$\frac{\eta}{2\sqrt{s}} \|v_{k+1} - v_k\|_{\mathcal{L}}^2 = \frac{\eta}{2\sqrt{s}} \|x_k - y_k\|_{\mathcal{L}}^2 + \frac{\sqrt{s}}{2\eta} \|G'(y_k)\|_{\mathcal{L}^{-1}}^2 + \langle G'(y_k), y_k - x_k \rangle.$$

Proof. Combine (3.4) and the relations (5.1), and then use (3.2) to obtain

$$\begin{aligned} v_{k+1} - v_k &= x_k + \frac{1}{\theta}(x_{k+1} - x_k) + \frac{1}{\theta}x_k - \left(1 + \frac{1}{\theta}\right)y_k \\ &= x_k - y_k + \frac{1}{\theta}(x_{k+1} - y_k) = x_k - y_k - \frac{\sqrt{s}}{\eta}\mathcal{L}^{-1}G'(y_k). \end{aligned}$$

Take \mathcal{L} -norm square on both sides and then multiply by $\frac{\eta}{2\sqrt{s}}$. \square

We are now in a position to prove the main result of this section, the exponential convergence of PAGD using energy arguments. The following result and its consequences are another of the main contributions of this work. To state it, we recall that the Lyapunov function of (4.1) $E : \mathbb{H}^2 \rightarrow \mathbb{R}$ is defined in (4.8) and that E_0 is its value at the initial state as mentioned in (4.9).

Theorem 5.8 (exponential decay). *Let the objective $G : \mathbb{H} \rightarrow \mathbb{R}$ be locally Lipschitz smooth and μ -strongly convex. If PAGD, as described in Algorithm 2, is applied to approximate $x^* = \operatorname{argmin}_{x \in \mathbb{H}} G(x)$ with a step size satisfying (5.3), where $r > 1$, B is the invariant set given by (5.2), and L_B is the Lipschitz smoothness constant associated with B , then the Lyapunov function (4.8) decays exponentially along the iterates $\{x_k\}_{k \geq 0}$. More specifically, for $k \geq 0$, we have*

$$(5.17) \quad E(x_{k+1}, v_{k+1} - x^*) \leq (1 - \theta)E(x_k, v_k - x^*), \quad E(x_k, v_k - x^*) \leq (1 - \theta)^k E_0.$$

Proof. Define, for $k \geq 0$, $\mathcal{E}_k = (1 - \theta)^{-k} E(x_k, v_k - x^*)$, which is the discrete analogue of the exponentially inflated energy in the the proof of Theorem 4.4. To simplify notation, we set $C_{\theta,k} = (1 - \theta)^{-(k+1)} > 0$. Then, similarly to the ODE case, one can show the discrete time derivative of \mathcal{E}_k is nonpositive as follows. First, we simply use the forward difference time derivative, rearrange, and use Lemma 5.5 to get

$$\begin{aligned} \frac{\mathcal{E}_{k+1} - \mathcal{E}_k}{\sqrt{s}} &= \frac{1}{\sqrt{s}} \left[(1 - \theta)^{-(k+1)} \left(\frac{1}{\eta}(G(x_{k+1}) - G^*) + \frac{\eta}{2}\|v_{k+1} - x^*\|_{\mathcal{L}}^2 \right) \right. \\ &\quad \left. - (1 - \theta)^{-k} \left(\frac{1}{\eta}(G(x_k) - G^*) + \frac{\eta}{2}\|v_k - x^*\|_{\mathcal{L}}^2 \right) \right] \\ &= C_{\theta,k} \left[\frac{1}{\eta} \frac{G(x_{k+1}) - G(x_k)}{\sqrt{s}} + (G(x_k) - G^*) \right. \\ &\quad \left. + \frac{\eta}{2\sqrt{s}} (\|v_{k+1} - x^*\|_{\mathcal{L}}^2 - \|v_k - x^*\|_{\mathcal{L}}^2) + \frac{\eta^2}{2}\|v_k - x^*\|_{\mathcal{L}}^2 \right] \\ &\leq C_{\theta,k} \left[-\frac{\sqrt{s}}{2\eta}\|G'(y_k)\|_{\mathcal{L}^{-1}}^2 - \frac{\eta}{2\sqrt{s}}\|x_k - y_k\|_{\mathcal{L}}^2 + (G(x_k) - G^*) \right. \\ &\quad \left. + \frac{1}{\theta}\langle G'(y_k), y_k - x_k \rangle + \frac{\eta}{2\sqrt{s}} (\|v_{k+1} - x^*\|_{\mathcal{L}}^2 - \|v_k - x^*\|_{\mathcal{L}}^2) \right. \\ &\quad \left. + \frac{\eta^2}{2}\|v_k - x^*\|_{\mathcal{L}}^2 \right]. \end{aligned}$$

We continue by using Lemma 5.6 and then Lemma 5.7, then it follows

$$\begin{aligned}
\frac{\mathcal{E}_{k+1} - \mathcal{E}_k}{\sqrt{s}} &\leq C_{\theta,k} \left[-\frac{\sqrt{s}}{2\eta} \|G'(y_k)\|_{\mathcal{L}^{-1}}^2 - \left(\frac{\eta}{2\sqrt{s}} + \frac{1}{2s}\right) \|x_k - y_k\|_{\mathcal{L}}^2 + (G(x_k) - G^*) \right. \\
&\quad \left. + \frac{\eta}{2\sqrt{s}} \|v_{k+1} - v_k\|_{\mathcal{L}}^2 + \frac{\eta^2}{2} \|y_k - x^*\|_{\mathcal{L}}^2 + \langle G'(y_k), x^* - y_k \rangle \right] \\
&= C_{\theta,k} \left[-\frac{1}{2s} \|y_k - x_k\|_{\mathcal{L}}^2 + (G(x_k) - G^*) + \langle G'(y_k), y_k - x_k \rangle \right. \\
&\quad \left. + \langle G'(y_k), x^* - y_k \rangle + \frac{\eta^2}{2} \|y_k - x^*\|_{\mathcal{L}}^2 \right].
\end{aligned}$$

Finally, add and subtract $G(y_k)$ from the last expression, and use the following estimates, which are simple rearrangements of the lower and upper quadratic traps,

$$\begin{aligned}
G(y_k) - G^* + \langle G'(y_k), x^* - y_k \rangle &\leq -\frac{\mu}{2} \|y_k - x^*\|_{\mathcal{L}}^2 \\
G(x_k) - G(y_k) + \langle G'(y_k), y_k - x_k \rangle &\leq \frac{L_B}{2} \|x_k - y_k\|_{\mathcal{L}}^2,
\end{aligned}$$

then we arrive at

$$\begin{aligned}
\frac{\mathcal{E}_{k+1} - \mathcal{E}_k}{\sqrt{s}} &\leq C_{\theta,k} \left[G(x_k) - G(y_k) + \langle G'(y_k), y_k - x_k \rangle + G(y_k) - G^* \right. \\
&\quad \left. + \langle G'(y_k), x^* - y_k \rangle - \frac{1}{2s} \|y_k - x_k\|_{\mathcal{L}}^2 + \frac{\eta^2}{2} \|y_k - x^*\|_{\mathcal{L}}^2 \right] \\
&\leq C_{\theta,k} \left[\frac{1}{2} \left(L_B - \frac{1}{s} \right) \|y_k - x_k\|_{\mathcal{L}}^2 \right].
\end{aligned}$$

The step size condition forces the last term to be nonpositive. Therefore, we conclude that $\{\mathcal{E}_k\}_{k \geq 0}$ is nonincreasing, from which we obtain (5.17). \square

The following estimates are evident.

Corollary 5.9 (rate of convergence). *In the setting of Theorem 5.8, we have that the iterates of PAGD, as described in Algorithm 2, converge to x^* , the minimizer of G , at an exponential rate. More specifically, for a suitable $r > 1$ the step size can be set $s = 1/L_B$ and, in this case, for $k \geq 0$,*

$$(5.18) \quad \frac{1}{\eta} (G(x_k) - G^*) + \frac{\eta}{2} \|v_k - x^*\|_{\mathcal{L}}^2 \leq (1 - \sqrt{\rho})^k E_0,$$

which implies

$$(5.19) \quad G(x_k) - G^* \leq (1 - \sqrt{\rho})^k \eta E_0, \quad \|x_k - x^*\|_{\mathcal{L}} \leq (1 - \sqrt{\rho})^{\frac{k}{2}} \sqrt{\frac{2E_0}{\eta}}.$$

Furthermore, we have exponential convergence in the \mathcal{L}^{-1} -norm of the residuals: for $k \geq 0$,

$$(5.20) \quad \|G'(y_k)\|_{\mathcal{L}^{-1}} \leq 3L_B \sqrt{\frac{2E_0}{\eta}} (1 - \sqrt{\rho})^{\frac{k-1}{2}}.$$

Proof. We can choose an appropriate $r > 1$ so that the step size condition (5.3) reduces to $s \in (0, L_B^{-1}]$; see Remark 5.3. Estimate (5.18) and the first estimate of

(5.19) follow from (5.17) upon setting $s = 1/L_B$. The second estimate of (5.19) follows by applying strong convexity of G to the first estimate of (5.19).

Next, from the estimate (5.13), one obtains

$$(5.21) \quad G^* \leq G(x_{k+1}) \leq G(y_k) - \frac{1}{2L_B} \|G'(y_k)\|_{\mathcal{L}^{-1}}^2,$$

from which, one obtains the following by rearranging and then using the upper quadratic trap

$$\|G'(y_k)\|_{\mathcal{L}^{-1}} \leq \sqrt{2L_B(G(y_k) - G^*)} \leq L_B \|y_k - x^*\|_{\mathcal{L}}.$$

In addition, we also have, from the definition of y_k and $0 < \lambda < 1$,

$$\|y_k - x^*\|_{\mathcal{L}} = \|x_k - x^* + \lambda(x_k - x_{k-1} \pm x^*)\|_{\mathcal{L}} \leq 2\|x_k - x^*\|_{\mathcal{L}} + \|x_{k-1} - x^*\|_{\mathcal{L}}.$$

Combining the last two estimates and using (5.19), we obtain (5.20). \square

Remark 5.10 (total energy). The exponential decrease of the “total energy” at every step, given in (5.18), does not imply that the “potential energy” $G(x_{k+1}) - G^*$ or the “kinetic energy” $\frac{\mu}{2} \|v_{k+1} - x^*\|_{\mathcal{L}}^2$ decay monotonically by themselves. Corollary 5.9 only asserts exponential bounds. The same is true for the decay of the \mathcal{L}^{-1} -norm of the residuals $\|G'(y_k)\|_{\mathcal{L}^{-1}}$. In fact, the numerical illustrations of Section 6 show that these quantities may oscillate. \blacksquare

Remark 5.11 (matching convergence rates). As discussed in Section 3, in the case of G being locally Lipschitz smooth, μ -strongly convex, the (best) contraction factor for PGD is $(\frac{1-\rho}{1+\rho})^2$ while we have $1 - \sqrt{\rho}$ for PAGD (see Theorem 5.8), where we recall $\rho = \mu/L_B$ and $L_B > 0$ is the Lipschitz smoothness constant on some appropriate invariant set B . It must be pointed out that this rate for PGD is achieved by choosing a “particularly good” step size that is only available to PGD: $s = \frac{2}{L_B + \mu}$ (see [17, Theorem 2.1.15]). More specifically, we have a contraction factor $1 - s \frac{2\mu L_B}{L_B + \mu}$ for PGD provided $0 < s \leq \frac{2}{L_B + \mu}$. If one uses the step size $s = 1/L_B$, then the contraction factor for PGD turns out to be $\frac{1-\rho}{1+\rho}$. This choice makes it easier to see the rate match the continuous time model. Setting $p = 2$ in [22, SI (Supplement Information) Theorem H.2] we get that the gradient flow

$$\dot{X} = -\mathcal{L}^{-1}G'(X)$$

has convergence rate $G(X(t)) - G^* \leq (G(X(0)) - G^*)e^{-\mu t}$. However, using an estimate available to μ -strongly convex functions, [17, Theorem 2.1.10 (2.1.19)], we can do better to get $G(X(t)) - G^* \leq (G(X(0)) - G^*)e^{-2\mu t}$ (Wibisono et al. did not use an optimal constant for the case of $p = 2$ in the proof in order to incorporate a more general notion of strong convexity). Then, we see that setting $t = sk$ and $s = 1/L_B$ for the gradient flow, and assuming $\rho \ll 1$, the contraction factor can be approximated by

$$e^{-2\mu s} \approx 1 - 2\mu s = 1 - 2\rho,$$

which is close to $\frac{1-\rho}{1+\rho}$. Similarly, setting $t = \sqrt{s}k$ and $s = 1/L_B$ in (4.13) and referring to Corollary 5.9, we have the contraction factors

$$e^{-\sqrt{\mu s}} \approx 1 - \sqrt{\mu s} = 1 - \sqrt{\rho}$$

for the IVP (4.1), which matches that of PAGD. \blacksquare

6. NUMERICAL EXPERIMENTS

In this section, we carry out a series of numerical experiments aimed at illustrating the theory that we have developed. In all our examples, we approximate the solution to the nonlinear PDE (6.1) by iteratively minimizing an energy related to this PDE. The approximate solution is computed using a pseudo-spectral method [7, 20], which was implemented in an in-house Matlab R2016a© code. This pseudo-spectral code heavily uses the built-in `fft` and `ifft` Matlab internal routines to invert preconditioners and apply residuals.

The energy minimization is carried out with either GD, AGD, PGD, or PAGD, where the algorithms stop if either:

- (a) the ∞ -norm (when the true solution is unknown) or the \mathcal{L}_N -norm (when the true solution is known) of the search direction is smaller than a certain tolerance, which we will call *convergence*;
- (b) the norm being measured is larger than a certain upper tolerance, which we will call *blow up*;
- (c) the number of iterations reaches a certain number, which we will call *no convergence*.

In the conditions above, we mean by “search directions” the residual if the scheme does not involve a preconditioner. If the scheme involves a (discrete) preconditioner \mathcal{L}_N (see (6.19) for definition), the search direction is the solution to $\mathcal{L}_N s = r$, where r is the residual. In all implementations, the initial guess is always zero.

6.1. The continuous problem. To test the performance of our schemes, we will approximate the solution to the following “nonlocal” PDE:

$$(6.1) \quad (-\Delta)^\alpha u + |u|^{p-2}u + tu = f \quad \text{in } \Omega = (0, 1)^2 \subset \mathbb{R}^2,$$

supplemented with periodic boundary conditions. Here $\alpha > 0$, $p \geq 2$, and $t > 0$. Here and in what follows, all functions are real-valued except for the exponential functions appearing in Fourier series and Fourier coefficients. The nonlocal operator $(-\Delta)^\alpha$ is the *spectral* fractional Laplacian, which is defined via Fourier series as explained below.

For every $v \in L^2_{\text{per}}(\Omega)$ we have that

$$v(\mathbf{x}) = \sum_{\mathbf{m} \in \mathbb{Z}^2} \hat{v}_{\mathbf{m}} e^{2\pi i \mathbf{m} \cdot \mathbf{x}},$$

where the equality is in the $L^2(\Omega)$ -sense, $\mathbf{x} = (x, y) \in \bar{\Omega}$, $i = \sqrt{-1}$, and

$$\hat{v}_{\mathbf{m}} = \int_{\Omega} v(\mathbf{x}) e^{-2\pi i \mathbf{m} \cdot \mathbf{x}} d\mathbf{x}, \quad \mathbf{m} \in \mathbb{Z}^2.$$

Thus, we define

$$(-\Delta)^\alpha v(\mathbf{x}) = \sum_{\mathbf{m} \in \mathbb{Z}^2} (4\pi^2 |\mathbf{m}|^2)^\alpha \hat{v}_{\mathbf{m}} e^{2\pi i \mathbf{m} \cdot \mathbf{x}},$$

provided that the sum is finite.

With this definition at hand, it is not difficult to see that (6.1) in its weak form, can be seen as the Euler-Lagrange equation for the functional

$$(6.2) \quad G(u) = \int_{\Omega} \left(\frac{1}{2} |(-\Delta)^{\frac{\alpha}{2}} u|^2 + \frac{1}{p} |u|^p + \frac{t}{2} |u|^2 - fu \right) d\mathbf{x},$$

over the space $\mathbb{H} = H_{\text{per}}^\alpha(\Omega) \cap L^p(\Omega)$, that is, the space of periodic, p -integrable functions, whose α -order derivatives in the Fourier sense are also square integrable. It is well known that $\{e^{2\pi i \mathbf{m} \cdot \mathbf{x}}\}_{\mathbf{m} \in \mathbb{Z}^2}$ is an orthonormal basis of $L_{\text{per}}^2(\Omega)$. Then, \mathbb{H} can be equivalently defined via

$$(6.3) \quad \mathbb{H} = \left\{ v \in L_{\text{per}}^p(\Omega) \left| \sum_{\mathbf{m} \in \mathbb{Z}^2} |\mathbf{m}|^\alpha |\hat{v}_{\mathbf{m}}|^2 < \infty \right. \right\}.$$

The existence and uniqueness of a weak solution to (6.1) is guaranteed for any $f \in L_{\text{per}}^{p'}(\Omega)$, where $1/p + 1/p' = 1$, since, in this case, the energy is well-defined, strictly convex, and coercive.

For the space \mathbb{H} to possess a Hilbert structure, a restriction on p must be imposed depending on α . For ease of notation, let (\cdot, \cdot) and $\|\cdot\|$ denote the $L^2(\Omega)$ -inner product and $L^2(\Omega)$ -norm respectively. A natural inner product on $H_{\text{per}}^\alpha(\Omega)$ is given by

$$(6.4) \quad (v, w)_{H_{\text{per}}^\alpha(\Omega)} = ((-\Delta)^{\frac{\alpha}{2}} v, (-\Delta)^{\frac{\alpha}{2}} w) + (v, w),$$

and its associated norm by $\|v\|_{H_{\text{per}}^\alpha(\Omega)} = \sqrt{(v, v)_{H_{\text{per}}^\alpha(\Omega)}}$. The following is a standard Sobolev embedding result. For a proof, see, e.g., [1, Theorem 7.34].

Proposition 6.1 (Sobolev embedding). *Let $\alpha \in (0, 1]$. For all $p \in [2, p^*]$ with $p^* = \frac{2}{1-\alpha}$ if $\alpha < 1$ or $p \in [2, \infty)$ if $\alpha = 1$, there exists $C_{\text{emb}} = C_{\text{emb}}(p, \alpha) > 0$ such that, for all $v \in H_{\text{per}}^\alpha(\Omega)$,*

$$(6.5) \quad \|v\|_{L^p(\Omega)} \leq C_{\text{emb}} \|v\|_{H_{\text{per}}^\alpha(\Omega)}.$$

We introduce the preconditioner

$$(6.6) \quad \mathcal{L}u = (-\Delta)^\alpha u + \nu u,$$

where $\nu \geq 0$ is a free parameter. Note that the action of this preconditioner needs to be understood variationally, that is,

$$\langle \mathcal{L}u, v \rangle = \int_{\Omega} ((-\Delta)^{\frac{\alpha}{2}} u (-\Delta)^{\frac{\alpha}{2}} v + \nu uv) \, d\mathbf{x}.$$

Remark 6.2 (notation). As it is clear from its definition, the Lipschitz constant of G' depends on the norm being used. Thus, we will make a difference between the case with preconditioner and without it. \hat{L} denotes the Lipschitz constant with respect to the preconditioner-induced norm $\|\cdot\|_{\mathcal{L}}$, while L is the constant with respect to the original norm $\|\cdot\|_{\mathbb{H}}$. \blacksquare

We investigate the properties of G in the following result.

Proposition 6.3 (properties of G). *Let G be given by (6.2) and the preconditioner \mathcal{L} by (6.6). Then, G is strongly convex with respect to \mathcal{L} -norm. If, in addition, p satisfies the conditions of Proposition 6.1, then G is locally Lipschitz smooth with respect to \mathcal{L} -norm.*

Proof. First, the action of G' is characterized by the following: for $v, w \in \mathbb{H}$,

$$\langle G'(v), w \rangle = ((-\Delta)^{\frac{\alpha}{2}} v, (-\Delta)^{\frac{\alpha}{2}} w) + t(v, w) + (|v|^{p-2} v, w) - (f, w).$$

Note also that the following estimates hold, which are a special case of [3, Lemma 2.1]: for $p > 1$, there exist $C_{p1}, C_{p2} > 0$, which depend only on p , such that for all $\xi, \eta \in \mathbb{R}$,

$$(6.7) \quad ||\xi|^{p-2}\xi - |\eta|^{p-2}\eta| \leq C_{p1}|\xi - \eta|(|\xi| + |\eta|)^{p-2},$$

$$(6.8) \quad (|\xi|^{p-2}\xi - |\eta|^{p-2}\eta)(\xi - \eta) \geq C_{p2}|\xi - \eta|^2(|\xi| + |\eta|)^{p-2}.$$

Thus, using (6.8)

$$\begin{aligned} & \langle G'(v) - G'(w), v - w \rangle \\ &= \|(-\Delta)^{\frac{\alpha}{2}}(v - w)\|^2 + t\|v - w\|^2 + (|v|^{p-2}v - |w|^{p-2}w, v - w) \\ &\geq \|(-\Delta)^{\frac{\alpha}{2}}(v - w)\|^2 + t\|v - w\|^2 \geq \hat{\mu}\|v - w\|_{\mathcal{L}}^2, \end{aligned}$$

where

$$(6.9) \quad \hat{\mu} = \min\{1, t/\nu\}.$$

Observe that this holds without referring to Sobolev embedding. Note also that this implies the coercivity of G with respect to \mathcal{L} -norm, that is, $\lim_{\|v\|_{\mathcal{L}} \rightarrow \infty} G(v) = \infty$.

Next, thanks to coercivity, for any bounded, convex set $B \subset \mathbb{H}$ there exists $M_B \in \mathbb{R}$ such that $B \subset \{x \in \mathbb{H} \mid G(x) \leq M_B\}$. Hence, for each $v \in B$, using Cauchy-Schwarz inequality and Young's inequality, it follows that there exists $\varepsilon > 0$ such that

$$\begin{aligned} M_B \geq G(v) &= \frac{1}{2}\|(-\Delta)^{\frac{\alpha}{2}}v\|^2 + \frac{1}{p}\|v\|_{L^p(\Omega)}^p + \frac{t}{2}\|v\|^2 - (f, v) \\ (6.10) \quad &\geq \frac{1}{2}\|(-\Delta)^{\frac{\alpha}{2}}v\|^2 + \frac{1}{p}\|v\|_{L^p(\Omega)}^p + \frac{t}{4}\|v\|^2 - \frac{1}{2\varepsilon}\|f\|^2. \end{aligned}$$

Rearranging this, we see that there exists $C_{f,t,p,B} > 0$ such that

$$(6.11) \quad \|v\|_{L^p(\Omega)} \leq C_{f,t,p,B} \quad \forall v \in B.$$

On the other hand, using (6.7), Hölder's inequality, and (6.11), we have, for all $v, w \in B$,

$$\begin{aligned} & \langle G'(v) - G'(w), v - w \rangle \\ &= \|(-\Delta)^{\frac{\alpha}{2}}(v - w)\|^2 + t\|v - w\|^2 + (|v|^{p-2}v - |w|^{p-2}w, v - w) \\ &\leq \|(-\Delta)^{\frac{\alpha}{2}}(v - w)\|^2 + t\|v - w\|^2 + C_{p1} \int_{\Omega} |v - w|^2(|v| + |w|)^{p-2} d\mathbf{x} \\ &\leq \|(-\Delta)^{\frac{\alpha}{2}}(v - w)\|^2 + t\|v - w\|^2 + C_{p3} \int_{\Omega} |v - w|^2(|v|^{p-2} + |w|^{p-2}) d\mathbf{x} \\ &\leq \|(-\Delta)^{\frac{\alpha}{2}}(v - w)\|^2 + t\|v - w\|^2 + C_{p3}\|v - w\|_{L^p(\Omega)}^2 \left(\|v\|_{L^p(\Omega)}^{p-2} + \|w\|_{L^p(\Omega)}^{p-2} \right) \\ &\leq \|(-\Delta)^{\frac{\alpha}{2}}(v - w)\|^2 + t\|v - w\|^2 + 2C_{f,t,p,B}^{p-2} C_{p3}\|v - w\|_{L^p(\Omega)}^2, \end{aligned}$$

where $C_{p3} > 0$ is a constant reflecting the equivalence between $(|v| + |w|)^{p-2}$ and $|v|^{p-2} + |w|^{p-2}$.

Finally, owing to the restriction on p , Proposition 6.1 guarantees that

$$\|v - w\|_{L^p(\Omega)}^2 \leq C_{emb}^2 \|v - w\|_{H_{\text{per}}^{\alpha}(\Omega)}^2,$$

so that

$$\langle G'(v) - G'(w), v - w \rangle \leq \hat{L}_B \|(v - w)\|_{\mathcal{L}}^2,$$

with $\hat{L}_B = \max\{1, t/\nu, 2C_{f,t,p,B}^{p-2}C_{p3}C_{emb}^2\}$. \square

Remark 6.4 (strong Lipschitz smoothness). The proof of Proposition 6.3 can be easily modified to show that G is locally Lipschitz smooth in the strong sense, i.e., (2.10) holds.

6.2. Discretization. We discretize the model problem (6.1) by introducing a uniform grid of points. To simplify the presentation, we choose $N \in \mathbb{N}$ with $N = 2K+1$ for some integer $K \geq 1$. (The details for the case that N is even are only slightly more complicated.) Define $h = 1/N$, and introduce the grid domain

$$\Omega_N = \{(x_\ell, y_m) \in [0, 1]^2 \mid x_\ell = \ell h, y_m = mh, 0 \leq \ell, m \leq N\}.$$

For ease of notation, let us introduce

$$\begin{aligned} \mathbb{N}_N^2 &= \{\mathbf{m} = (m_1, m_2) \in \mathbb{Z}^2 \mid 1 \leq m_1, m_2 \leq N\}, \\ \mathbb{Z}_K^2 &= \{\mathbf{r} = (r_1, r_2) \in \mathbb{Z}^2 \mid -K \leq r_1, r_2 \leq K\}. \end{aligned}$$

Then, for $\mathbf{m} \in \mathbb{N}_N^2$, we can denote $\mathbf{x}_\mathbf{m} = (x_{m_1}, y_{m_2}) \in \Omega_N$. This notation must not be confused with that of the iterates of PAGD.

Define the space of periodic grid functions

$$\mathbb{H}_N = \{v_N : \Omega_N \rightarrow \mathbb{R} \mid v_N(0, hm) = v_N(hN, hm), v_N(h\ell, 0) = v_N(h\ell, hN), \\ (6.12) \quad 0 \leq m, \ell \leq N\},$$

which we endow with the following L_N^2 -inner product

$$(6.13) \quad (v_N, w_N)_N = h^2 \sum_{\mathbf{m} \in \mathbb{N}_N^2} v_N(\mathbf{x}_\mathbf{m}) w_N(\mathbf{x}_\mathbf{m}),$$

and its associated norm $\|w_N\|_N = \sqrt{(w_N, w_N)_N}$. More generally, for $p \geq 1$,

$$\|w_N\|_{N,p} = \left(h^2 \sum_{\mathbf{m} \in \mathbb{N}_N^2} |w_N(\mathbf{x}_\mathbf{m})|^p \right)^{\frac{1}{p}}.$$

Given $w_N \in \mathbb{H}_N$, its *discrete Fourier transform* (DFT) is

$$\hat{w}_K(\mathbf{r}) = h^2 \sum_{\mathbf{s} \in \mathbb{N}_N^2} w_N(\mathbf{x}_\mathbf{s}) e^{-2\pi i \mathbf{r} \cdot \mathbf{x}_\mathbf{s}}, \quad \mathbf{r} \in \mathbb{Z}_K^2.$$

We define the *discrete fractional Laplacian* $(-\Delta_N)^\alpha : \mathbb{H}_N \rightarrow \mathbb{H}_N$ by

$$(6.14) \quad [(-\Delta_N)^\alpha w_N](\mathbf{x}_\mathbf{m}) = \sum_{\mathbf{r} \in \mathbb{Z}_K^2} (4\pi^2 |\mathbf{r}|^2)^\alpha \hat{w}_K(\mathbf{r}) e^{2\pi i \mathbf{r} \cdot \mathbf{x}_\mathbf{m}}.$$

We define, for $v_N, w_N \in \mathbb{H}_N$, the H_N^α -inner product by

$$(6.15) \quad (v_N, w_N)_{H_N^\alpha} = (v_N, w_N)_N + ((-\Delta_N)^{\frac{\alpha}{2}} v_N, (-\Delta_N)^{\frac{\alpha}{2}} w_N)_N,$$

and $\|w_N\|_{H_N^\alpha} = \sqrt{(w_N, w_N)_{H_N^\alpha}}$.

We comment that there are, at least, three different natural choices for an inner product in \mathbb{H}_N : the L_N^2 -inner product (6.13), the H_N^α -inner product (6.15), and the \mathcal{L}_N -inner product (6.20), to be defined below. We will choose the first option, i.e., the L_N^2 -inner product. There are two reasons for this. First, it is more practical than the others, since the Euclidean setting is more common in classical linear algebra. Since the characterization of \mathbb{H}_N does not involve derivatives in any sense,

it is isomorphic to a Euclidean space of dimension $\mathfrak{d} = N^2$. Since the L_N^2 -norm is a scaled version of the $\ell^2(\mathbb{R}^{\mathfrak{d}})$ -norm, it should be more natural than the other options. This choice leads to the truly *non-preconditioned* schemes such as GD or AGD with which practitioners would be familiar. Moreover, it is practical since we can identify \mathbb{H}'_N with \mathbb{H}_N at no cost. When we implement the minimizing algorithms introduced in this paper, we need to find the representer of the residual with respect to the inner product that is being used. Although the H_N^α -inner product may seem more natural from a theoretical perspective, finding a representer of the residual with respect to this inner product involves solving another subproblem that is as costly as inverting the preconditioner (6.19). On the other hand, obtaining the representer of the residual with respect to the L_N^2 -inner product is free as long as we use grid functions in the strong form. For example, if we want to calculate $(v_N, (-\Delta)_N^\alpha w_N)_N$, we simply find $(-\Delta)_N^\alpha w_N$ according to the definition of the fractional Laplacian (6.14) and take L_N^2 -inner product. Secondly, it illustrates the effect of preconditioning more vividly. The comments after Theorem 6.7 explain this in detail.

Proposition 6.5 (Parseval). *Let $\alpha, \beta \geq 0$. For grid functions $v_N, w_N \in \mathbb{H}_N$, let $v = I_K(v_N), w = I_K(w_N) \in \mathcal{P}_K$, where \mathcal{P}_K is the space of Ω -periodic trigonometric polynomials of degree at most K and $I_K : \mathbb{H}_N \rightarrow \mathcal{P}_K$ maps a grid function, v_N , to a (unique) trigonometric polynomial, $v = I_K(v_N)$, that interpolates v_N , i.e., $v_N(\mathbf{x}_m) = v(\mathbf{x}_m)$ for all $\mathbf{x}_m \in \Omega_N$. Then,*

$$((-\Delta_N)^\alpha v_N, (-\Delta_N)^\beta w_N)_N = ((-\Delta)^\alpha v, (-\Delta)^\beta w).$$

Consequently,

$$(6.16) \quad \|v_N\|_{H_N^\alpha} = \|I_K(v_N)\|_{H_{\text{per}}^\alpha(\Omega)}.$$

Proof. This is a direct consequence of the orthonormality of $\{e^{2\pi i \mathbf{n} \cdot \mathbf{x}_m}\}_{\mathbf{n} \in \mathbb{Z}_K^2} \subset \mathbb{H}_N$ with respect to $(\cdot, \cdot)_N$ and that of $\{e^{2\pi i \mathbf{n} \cdot \mathbf{x}}\}_{\mathbf{n} \in \mathbb{Z}_K^2} \subset \mathcal{P}_K$ with respect to (\cdot, \cdot) once we realize that $v(\mathbf{x}) = I_K(v_N)(\mathbf{x}) = \sum_{\mathbf{r} \in \mathbb{Z}_K^2} \hat{v}_K(\mathbf{r}) e^{2\pi i \mathbf{r} \cdot \mathbf{x}}$ and that the same relation holds between w and w_N . \square

After having introduced all this notation, we can write our discrete problem as: given $f_N \in \mathbb{H}_N$, find $u_N \in \mathbb{H}_N$ such that

$$(6.17) \quad (-\Delta_N)^\alpha u_N + |u_N|^{p-2} u_N + t u_N = f_N.$$

Or, equivalently, for all $v_N \in \mathbb{H}_N$

$$((-\Delta_N)^{\frac{\alpha}{2}} u_N, (-\Delta_N)^{\frac{\alpha}{2}} v_N)_N + (|u_N|^{p-2} u_N, v_N)_N + t(u_N, v_N)_N = (f_N, v_N)_N.$$

In this problem, $f_N \in \mathbb{H}_N$ is some approximation of the problem data f . For example, if f is continuous, $f_N(\mathbf{x}_m) = f(\mathbf{x}_m)$ is a natural option, and if f is only an $L^2(\Omega)$ -function, then the sampling at the nodes of the $L^2(\Omega)$ -projection of f onto \mathcal{P}_K , the trigonometric polynomial of degree at most K , is natural although these two may not agree even if one starts with the same continuous function f . In fact, the difference between these two possibilities is very small if f is smooth and its derivatives are periodic [7, pp. 44–45].

Our discrete problem has a similar energy structure to the continuous problem. It is the Euler-Lagrange equation of the following functional

$$(6.18) \quad G_N(v_N) = \frac{1}{2} \|(-\Delta_N)^{\frac{\alpha}{2}} v_N\|_N^2 + \frac{1}{p} \|v_N\|_{N,p}^p + \frac{t}{2} \|v_N\|_N^2 - (f_N, v_N)_N.$$

We introduce a (discrete) preconditioner

$$(6.19) \quad \mathcal{L}_N = (-\Delta_N)^\alpha + \nu_N \text{id}_N,$$

where $\nu_N > 0$ and $\text{id}_N : \mathbb{H}_N \rightarrow \mathbb{H}_N$ is the identity map. The parameter $\nu_N > 0$ will be determined later. This preconditioner induces an inner product on \mathbb{H}_N given by

$$(6.20) \quad (v_N, w_N)_{\mathcal{L}_N} = \nu_N (v_N, w_N)_N + ((-\Delta_N)^{\frac{\alpha}{2}} v_N, (-\Delta_N)^{\frac{\alpha}{2}} w_N)_N,$$

and an associated norm $\|v_N\|_{\mathcal{L}_N} = \sqrt{(v_N, v_N)_{\mathcal{L}_N}}$. It is desirable that the convergence of our scheme does not deteriorate as we refine the grid points. We can ensure this under a certain restriction on p . The following proposition provides an important tool for that purpose.

Proposition 6.6 (discrete Sobolev embedding). *Let $\alpha \in (0, 1]$. For all $p \in [2, p^*]$ with $p^* = \frac{2}{1-\alpha}$ if $\alpha < 1$ or for all $p \in [2, \infty)$ if $\alpha = 1$, there exists a constant $C_{p,\alpha} > 0$ such that, for all $v_N \in \mathbb{H}_N$,*

$$(6.21) \quad \|v_N\|_{N,p} \leq C_{p,\alpha} \|v_N\|_{H_N^\alpha}.$$

$C_{p,\alpha}$ is independent of v_N and N .

Proof. It is well-known that, in our setting, the stability of the norm $\|\cdot\|_{N,p}$, is guaranteed. That is, there exists a constant C , which depends only on the dimension of Ω , such that $\|v_N\|_{N,p} \leq C \|v\|_{L^p(\Omega)}$ for all $v_N \in \mathbb{H}_N$; see, for instance, [14, Lemma 2.48], where $v = I_K(v_N)$ as introduced in Proposition 6.5. In conjunction with the Sobolev embedding at the continuous level, (6.5), and the Parseval's identity, (6.16), we have, for any $v_N \in \mathbb{H}_N$,

$$\|v_N\|_{N,p} \leq C \|v\|_{L^p(\Omega)} \leq C C_{p,\alpha} \|v\|_{H_{\text{per}}^\alpha(\Omega)} = C C_{p,\alpha} \|v_N\|_{H_N^\alpha}. \quad \square$$

The following result addresses dimension-independence of the (inverse) condition number as well as the structure of G_N that is needed to apply the theory we have developed in Section 5. Note that, in the following statement, the sublevel sets of G_N provide a compatible way to describe bounded, convex sets when we consider multiple resolutions since, strictly speaking, for different values of N , functions in \mathbb{H}_N may not be directly comparable.

Theorem 6.7 (properties of G_N). *Let the space of grid functions \mathbb{H}_N be given by (6.12) and the preconditioner \mathcal{L}_N by (6.19). Then, the energy functional $G_N : \mathbb{H}_N \rightarrow \mathbb{R}$ defined by (6.18) is strongly convex and locally Lipschitz smooth with respect to the \mathcal{L}_N -norm. Moreover, the strong convexity constant $\hat{\mu}_N$ is independent of N . Suppose, in addition, that p satisfies the conditions of Proposition 6.6 and that f_N is defined in a stable manner when we pose the discrete problem (6.17), i.e., there exists $C > 0$ independent of N such that*

$$\|f_N\|_{N,2} \leq C \|f\|_{L^2(\Omega)}.$$

Then, the local Lipschitz smoothness constant \hat{L}_N is also independent of N in the sense that, for each $M \in \mathbb{R}$, G_N is \hat{L}_N -Lipschitz smooth on the sublevel set

$$\{v_N \in \mathbb{H}_N \mid G(v_N) \leq M\}$$

with \hat{L}_N independent of N . Consequently, the (inverse) condition number $\hat{\mu}_N/\hat{L}_N$ with respect to the \mathcal{L}_N -norm stays away from 0 as $N \rightarrow \infty$.

Proof. The proof of the strong convexity is exactly parallel to that of Proposition 6.3. The proof of local Lipschitz smoothness is also parallel, but we need the assumed stability of $\|f_N\|_{N,2}$ to proceed from (6.10) to (6.11). Finally, to complete the proof, we simply replace the embedding constant C_{emb} with its discrete counterpart $C_{p,\alpha}$ as given in Proposition 6.6. \square

Since the (inverse) condition number $\hat{\mu}_N/\hat{L}_N$ governs the rate of convergence of PAGD (Corollary 5.9), the previous theorem guarantees that one can achieve the same rate of convergence even if we refine the number of grid points $N \rightarrow \infty$. However, this is in terms of the number of iterations, and the wall clock time will take longer as the refinement is conducted.

Being in finite dimensions, G_N is also strongly convex, and locally Lipschitz smooth with respect to *any norm*, for instance $\|\cdot\|_N$. The constants in this case, however, are different and depend on the dimension of \mathbb{H}_N , which obviously depends on the number of grid points, and thus on N . We label them μ_N and L_N to distinguish them from the dimension-independent constants $\hat{\mu}_N$ and \hat{L}_N respectively.

6.3. A problem with a manufactured solution. In this first experiment, we solve (6.17) by minimizing the energy (6.18). To be able to compute the rate of energy decay, we manufacture a solution. Namely, we set

$$u_N(\mathbf{x}_m) = \exp\left(\sin 2\pi\left(x_{m_1} - \frac{1}{4}\right) + \sin 4\pi\left(y_{m_2} - \frac{3}{8}\right)\right),$$

so that the right hand side is

$$f_N(\mathbf{x}_m) = \sum_{\mathbf{r} \in \mathbb{Z}_K^2} (4\pi^2|\mathbf{r}|^2)^\alpha \hat{u}_K(\mathbf{r}) e^{2\pi i \mathbf{r} \cdot \mathbf{x}_m} + |u_N(\mathbf{x}_m)|^{p-2} u_N(\mathbf{x}_m) + t u_N(\mathbf{x}_m),$$

with $\alpha = 0.5$, $p = 4$, and $t = 1$.

We set $N = 64$ and found, experimentally, that the values $\nu_N = 1.2$, $\mu_N = 1$ are optimal, while we set $\hat{\mu}_N = 5/6 = \min\{1, t/\nu_N\}$ in view of (6.9). To specify step sizes, recall the step size rules that theoretically guarantee convergence (see Section 3): $s = 2/(L_N + \mu_N)$ for GD, $s = 1/L_N$ for AGD, $s = 2/(\hat{L}_N + \hat{\mu}_N)$ for PGD, and $s = 1/\hat{L}_N$ for PAGD. Step sizes are set by these relations with $L_N = 500$ and $\hat{L}_N = 20$, which are also experimentally proved to be optimal. However, it must be noted that this is just a way of setting step sizes. We do not really know neither whether the values for L_N or \hat{L}_N are the Lipschitz constants of the corresponding energy functionals nor whether the aforementioned step size rules give the optimal results even if we knew the Lipschitz constants. In fact, our last experiment suggests that larger step sizes than what is theoretically proven seem to work.

Figure 1 shows the performance of GD, AGD, PGD, and PAGD when used to solve (6.17) by minimizing (6.18), where the data is as described above. The stopping criteria take the following parameters: the tolerance is 10^{-8} , the upper tolerance is 10^{10} , and the maximum number of iterations is 200.

Figure 1 (A) shows the decay of the objective, $G_N(x_k) - G_N(u_N)$ which is, up to a constant, the same as the decay of the potential energy, for all four schemes. Here k is the number of iterations. Figure 1 (B) shows the decay of the \mathcal{L}_N -norm of the errors. Notice that PAGD performs significantly better than all the other methods.

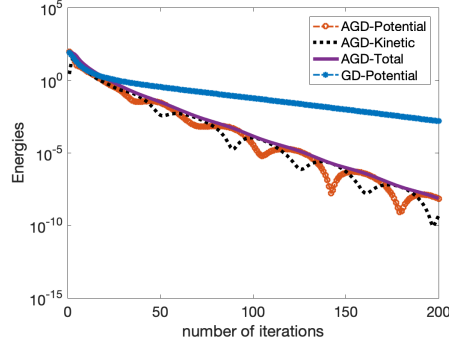
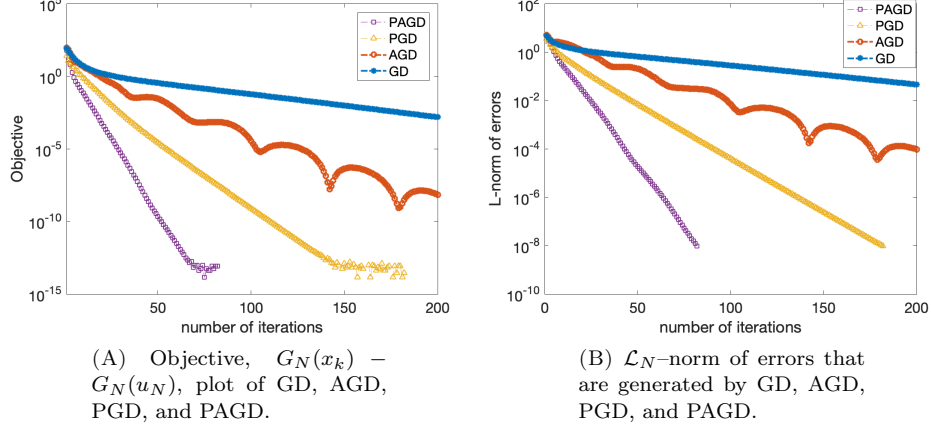


FIGURE 1. Objective, error, and energy decay plots for GD, AGD, PGD, and PAGD. They are implemented to solve (6.17) by minimizing (6.18) ($\alpha = 0.5$, $p = 4$, $t = 1$, $N = 64$, $\nu_N = 1.2$, $L_N = 500$, $\mu_N = 1$, $\hat{L}_N = 20$, $\hat{\mu}_N = 5/6 = \min\{1, t/\nu_N\}$, and step sizes are set via $s = 2/(L_N + \mu_N)$ for GD, $s = 1/L_N$ for AGD, $s = 2/(\hat{L}_N + \hat{\mu}_N)$ for PGD, and $s = 1/\hat{L}_N$ for PAGD). The vertical axes (logarithmic scale) show the value of the objective, \mathcal{L}_N -norm of errors, or various energies while the horizontal axis (linear scale) shows the number of iterations.

Figure 1 (C) shows the performance of GD and AGD. Since these schemes do not involve a preconditioner, the corresponding total energy is defined by

$$(6.22) \quad E_N(x_k, v_k) = \frac{1}{\eta_N} (G_N(x_k) - G_N(u_N)) + \frac{\eta_N}{2} \|v_k - u_N\|_N^2,$$

where k is the number of iterations and $\eta_N = \sqrt{\mu_N}$. The first and second terms can be understood as potential and kinetic energy respectively. Figure 1 (C) shows

the decay of various energies for nonpreconditioned schemes. This figure better illustrates our analysis of the previous section than the preconditioned ones since they converge slower. As expected, AGD performs substantially better than GD. The total energy of AGD decreases steadily and exponentially fast. Notice that the vertical axis is in logarithmic scale. This matches what is predicted by the theory in Theorem 5.8. Observe also that the potential and kinetic energies of AGD, by themselves, oscillate; see Remark 5.10. The physical analogy for AGD described in Remark 4.1 is clear from this picture. A fraction of the potential energy is converted to kinetic energy and they fluctuate as the mechanical system converges to equilibrium.

6.4. A problem where the solution is unknown. In this second experiment we, again, solve (6.17) by minimizing the energy (6.18). The discrete right hand side f_N is given by

$$(6.23) \quad f_N(\mathbf{x}_m) = \exp(\sin 2\pi(x_{m_1} - 0.25) + \sin 2\pi(y_{m_2} - 0.25)).$$

The parameters of the PDE are set to $\alpha = 0.5$, $p = 10$, and $t = 1$. Observe that for these values of α and p we do not have that $H_{\text{per}}^\alpha(\Omega) \hookrightarrow L^p(\Omega)$. We found, experimentally, that the choice $\nu_N = 0.9$ is optimal for the preconditioner. We also set $\mu_N = 1$ and $\hat{\mu}_N = 1 = \min\{1, t/\nu_N\}$ in view of (6.9) as before. Step sizes are set in the same way as in the previous experiment with $L_N = 300$ or 3000 , and $\hat{L}_N = 9$. The values of μ_N , L_N , and \hat{L}_N were experimentally found to be optimal except for $L_N = 3000$. That is, they yield the best convergence rate with all other parameters being fixed. A more detailed explanation about $L_N = 3000$ will follow. Two different degrees of resolution are used to show the dimension dependence of nonpreconditioned schemes. The stopping criterion parameters are as before.

Figure 2 shows the ∞ -norm of the search directions for GD, AGD, PGD, and PAGD with varying degrees of resolution and with two different step sizes for GD and AGD, which are determined by the same step size rules as in the previous experiment with $L_N \in \{300, 3000\}$. In Figure 2 (A), we observe a similar performance as in Figure 1. Recall that we do not have Sobolev embedding. Thus, one can expect the Lipschitz constant L_N , hence the step size, to depend on the number of grid points. In fact, theory predicts that even \hat{L}_N depends on it. However, for \hat{L}_N , such dependence is not observed within the range of N that we have chosen. We see that the step size for convergence indeed depends on N in Figure 2 (B). As we increase the resolution of the grid from $N = 64$ to $N = 512$, nonpreconditioned schemes become unstable. Figure 2 (C) shows that the stability of GD and AGD is recovered after L_N is increased from 300 to 3000, which amounts to decreasing the step size to roughly a tenth of the old one. ($L_N = 3000$ is not optimally chosen).

Figure 3 shows the dependence of L_N , hence the step size, on the number of grid points with the same experiment. However, here we use different tolerances and a different maximum number of iterations to best illustrate the dependence. For $N \in \{16, 32, 64, 128, 256, 512\}$, Figure 3 records the number of iterations for ∞ -norm of the search direction generated by each scheme to reach a tolerance 10^{-3} (“convergence”) or the maximum number of iterations, which is set to be 1000, if it does not reach the tolerance (“no convergence”). If the ∞ -norm of the search direction reaches an upper tolerance 10^8 , the algorithm records the number of iteration taken as 1100, which indicates “blowing up.” Figure 3 (A) shows when the step sizes of the nonpreconditioned schemes correspond to $L_N = 300$ and those

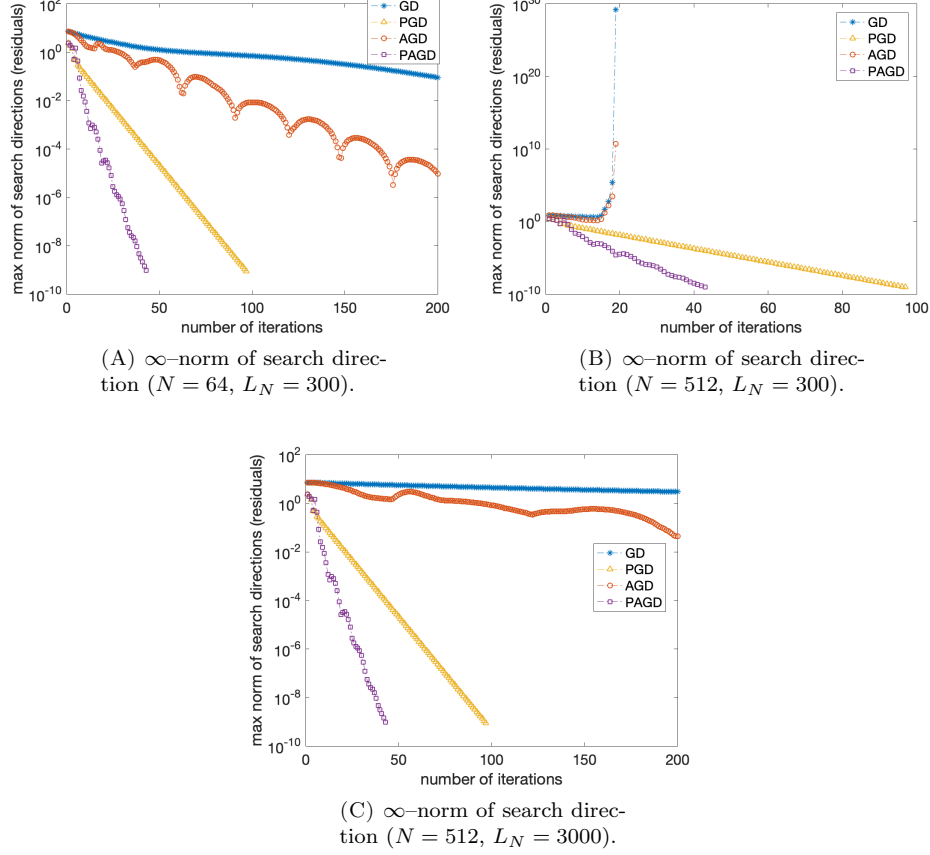


FIGURE 2. ∞ -norm plots of the search directions for GD, AGD, PGD, and PAGD. They are implemented to solve (6.17) by minimizing (6.18) with varying resolutions $N \in \{64, 512\}$ and varying step sizes for GD and AGD; $s = 2/(L_N + \mu_N)$ for GD and $s = 1/L_N$ for AGD with $L_N \in \{300, 3000\}$. The other parameters are set to $\alpha = 0.5$, $p = 10$, $t = 1$, $\nu_N = 0.9$, $\mu_N = 1$, $\hat{\mu}_N = 1 = \min\{1, t/\nu_N\}$, $s = 2/(\hat{L}_N + \hat{\mu}_N)$ for PGD, and $s = 1/\hat{L}_N$ for PAGD with $\hat{L}_N = 9$. The horizontal axis (linear scale) represents the number of iterations. The vertical axis (logarithmic scale) represents ∞ -norm of the search directions.

of the preconditioned ones correspond to $\hat{L}_N = 9$. GD and AGD converge until $N = 64$. However, they become unstable for $N \geq 128$. Figure 3 (B) shows the same experiment with smaller step sizes, which correspond to $L_N = 3000$. In this case, we recover the stability of GD and AGD.

6.5. A comparison between PGD and PAGD. In this final collection of experiments, we aim at comparing the performance of PGD and PAGD in different scenarios. To do so, we solve the discrete problem (6.17) by minimizing the energy

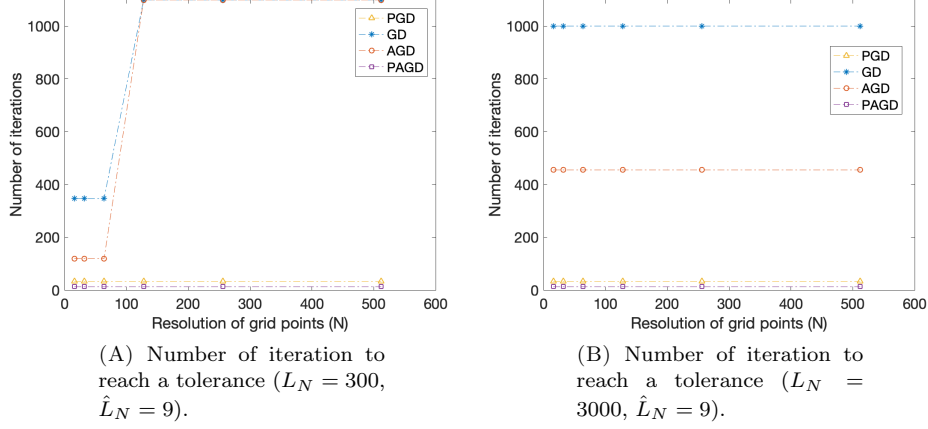


FIGURE 3. Number of iterations for ∞ -norm of the search directions to reach the tolerance 10^{-3} for GD, AGD, PGD, and PAGD. They are implemented to solve (6.17) by minimizing (6.18) with varying resolutions $N = 16, 32, 64, 128, 256, 512$ and varying $L_N = 300, 3000$ ($\alpha = 0.5$, $p = 10$, $t = 1$, $\nu_N = 0.9$, $\mu_N = 1$, L_N as indicated in the subfigures, $\hat{\mu}_N = 1 = \min\{1, t/\nu_N\}$, $\hat{L}_N = 9$). The horizontal axis represents the degrees of resolution, N . The vertical axis represents the minimum of the number of iterations for the ∞ -norm of the search directions to reach the tolerance 10^{-3} (convergence) or 1000 iterations. The number of iterations being 1100 means that the ∞ -norm of the search directions have reached the upper tolerance 10^8 (blow up).

(6.18) with the right hand side given by (6.23) as before. The problem parameters are set as $\alpha \in \{0.1j \mid j = 1, 2, 3, \dots, 10\} \cup \{1.5, 2.0, 2.5, 3.0\} \subset (0, 3]$, $p = 6$, and $t = 1$. We set $N = 64$ and $\hat{\mu}_N = \min\{1, t/\nu_N\}$. Then, for each value of α (column 1 of Table 1), PGD and PAGD are applied with $\nu_N \in \{0.1j \mid j = 1, 2, 3, \dots, 100\} \subset (0, 10]$ and the step size $s \in \{0.01j \mid j = 1, 2, 3, \dots, 200\} \subset (0, 2]$. Observe that neither Algorithm 1 nor Algorithm 2 require knowledge of \hat{L}_N a priori. Instead, we directly set the step size in this last experiment. Among these 20,000 possible values of ν_N and s , the minimal number of iterations for the ∞ -norm of the search direction generated by PGD and PAGD to reach a tolerance of 10^{-9} (convergence) is recorded (column 2 and column 5 of Table 1, respectively). A pair of values, ν_N and s , that led to the minimal number of iterations is also recorded (columns 3 and 4 of Table 1 for PGD and columns 6 and 7 of Table 1 for PAGD). There can be multiple such pairs. If this is the case, the pair (ν_N, s) that comes the first in the lexicographic order is recorded.

As we can see from Table 1, for the nonlocal PDE (6.17) with small α ($\alpha = 0.1, 0.2, 0.3, 0.4$), PAGD performs better than PGD when they are implemented with their own best pair of parameters ν_N and s among those pairs that were considered. In particular, in the cases of $\alpha = 0.1, 0.2, 0.3$, PAGD outperforms PGD while the best values of ν_N for the two schemes are similar, hence directly comparing their

α	PGD			PAGD		
	# iterations	ν_N	step size	# iterations	ν_N	step size
0.1	64	1.0	0.20	38	0.9	0.14
0.2	50	1.1	0.25	32	1.0	0.18
0.3	39	1.2	0.31	29	1.1	0.22
0.4	29	2.6	0.57	26	1.2	0.26
0.5	22	2.8	0.66	24	1.3	0.30
0.6	16	4.1	0.97	20	5.5	0.83
0.7	13	3.4	0.90	17	5.2	0.91
0.8	11	4.6	1.04	15	4.2	0.88
0.9	12	3.8	0.89	12	5.0	0.96
1.0	10	4.0	0.95	12	4.3	0.92
1.5	9	4.5	0.97	11	4.5	0.97
2.0	8	4.8	1.03	10	4.5	0.96
2.5	8	4.1	0.88	9	4.2	0.90
3.0	8	4.1	0.88	9	4.2	0.90

TABLE 1. The minimal number of iterations needed for the ∞ -norm of the search direction of PGD and PAGD to reach a tolerance of 10^{-9} and the values of ν_N and s (step size) that led to the minimum iterations for a range of values of α . They are implemented to solve (6.17) by minimizing the energy (6.18). $N = 64$, $\alpha \in \{0.1j \mid j = 1, 2, 3, \dots, 10\} \cup \{1.5, 2.0, 2.5, 3.0\} \subset (0, 3]$, $p = 6$, $t = 1$, $\hat{\mu}_N = \min\{1, t/\nu_N\}$, and f_N is given by (6.23). For each value of α , we consider $\nu_N \in \{0.1j \mid j = 1, 2, 3, \dots, 100\} \subset (0, 10]$ and $s \in \{0.01j \mid j = 1, 2, 3, \dots, 200\} \subset (0, 2]$. Among the possible 20,000 possible combinations of ν_N and s , we display the values that give the minimal number of iterations.

performances roughly make sense. An interesting thing, however, is that one cannot say that PAGD is *always* better than PGD. In fact, for the remaining values of α , PGD takes fewer iterations to converge in the aforementioned sense than PAGD provided they are equipped with their “best” parameters for each method. It must be noted that this result does not contradict our theory. The theory only tells us some upper bounds about the rate of convergence of the two schemes within a certain range of step size when they involve the same preconditioner. It does not explain what happens outside of that. The result provided here perhaps illustrates the latter case. In any case, we can see an improvement in the convergence of PAGD compared to PGD for “harder” problems ((6.17) with small α), where a stronger nonlocality is involved.

ACKNOWLEDGMENTS

SMW acknowledges partial financial support from NSF-DMS 1719854. AJS has been partially supported by NSF-DMS 1720123.

REFERENCES

- [1] Robert A. Adams and John J. F. Fournier. *Sobolev spaces*, volume 140 of *Pure and Applied Mathematics (Amsterdam)*. Elsevier/Academic Press, Amsterdam, second edition, 2003.
- [2] Zeyuan Allen-Zhu and Lorenzo Orecchia. Linear coupling: an ultimate unification of gradient and mirror descent. In *8th Innovations in Theoretical Computer Science Conference*, volume 67 of *LIPICs. Leibniz Int. Proc. Inform.*, pages Art. No. 3, 22. Schloss Dagstuhl. Leibniz-Zent. Inform., Wadern, 2017.
- [3] John W. Barrett and W. B. Liu. Finite element approximation of the p -Laplacian. *Math. Comp.*, 61(204):523–537, 1993.
- [4] Amir Beck. *First-order methods in optimization*, volume 25 of *MOS-SIAM Series on Optimization*. Society for Industrial and Applied Mathematics (SIAM), Philadelphia, PA; Mathematical Optimization Society, Philadelphia, PA, 2017.
- [5] Dimitri P. Bertsekas. *Nonlinear programming*. Athena Scientific Optimization and Computation Series. Athena Scientific, Belmont, MA, second edition, 1999.
- [6] Stephen Boyd and Lieven Vandenbergh. *Convex optimization*. Cambridge University Press, Cambridge, 2004.
- [7] C. Canuto, M. Y. Hussaini, A. Quarteroni, and T. A. Zang. *Spectral methods*. Scientific Computation. Springer-Verlag, Berlin, 2006. Fundamentals in single domains.
- [8] H. Cartan, J. Moore, D. Husemoller, and K. Maestro. *Differential Calculus on Normed Spaces: A Course in Analysis*. CreateSpace Independent Publishing Platform, 2017.
- [9] Long Chen, Xiaozhe Hu, and Steven M. Wise. Convergence analysis of the fast subspace descent methods for convex optimization problems, 2018.
- [10] Philippe G. Ciarlet. *Introduction to numerical linear algebra and optimisation*. Cambridge Texts in Applied Mathematics. Cambridge University Press, Cambridge, 1989. With the assistance of Bernadette Miara and Jean-Marie Thomas, Translated from the French by A. Buttigieg.
- [11] Philippe G. Ciarlet. *Linear and nonlinear functional analysis with applications*. Society for Industrial and Applied Mathematics, Philadelphia, PA, 2013.
- [12] Lawrence C. Evans. *Partial differential equations*, volume 19 of *Graduate Studies in Mathematics*. American Mathematical Society, Providence, RI, second edition, 2010.
- [13] Wenqiang Feng, Abner J. Salgado, Cheng Wang, and Steven M. Wise. Preconditioned steepest descent methods for some nonlinear elliptic equations involving p -Laplacian terms. *J. Comput. Phys.*, 334:45–67, 2017.
- [14] Boško S. Jovanović and Endre Süli. *Analysis of finite difference schemes*, volume 46 of *Springer Series in Computational Mathematics*. Springer, London, 2014. For linear partial differential equations with generalized solutions.
- [15] Hao Luo and Long Chen. From differential equation solvers to accelerated first-order methods for convex optimization. arXiv:1909.03145, 2019.
- [16] Yu. E. Nesterov. A method for solving the convex programming problem with convergence rate $O(1/k^2)$. *Dokl. Akad. Nauk SSSR*, 269(3):543–547, 1983.
- [17] Yurii Nesterov. *Introductory lectures on convex optimization*, volume 87 of *Applied Optimization*. Kluwer Academic Publishers, Boston, MA, 2004. A basic course.
- [18] Robert R. Phelps. *Convex functions, monotone operators and differentiability*, volume 1364 of *Lecture Notes in Mathematics*. Springer-Verlag, Berlin, second edition, 1993.
- [19] B. T. Poljak. Some methods of speeding up the convergence of iterative methods. *Ž. Vychisl. Mat i Mat. Fiz.*, 4:791–803, 1964.
- [20] Jie Shen, Tao Tang, and Li-Lian Wang. *Spectral methods*, volume 41 of *Springer Series in Computational Mathematics*. Springer, Heidelberg, 2011. Algorithms, analysis and applications.
- [21] Weijie Su, Stephen Boyd, and Emmanuel Candes. A differential equation for modeling nesterovs accelerated gradient method: Theory and insights. In Z. Ghahramani, M. Welling, C. Cortes, N. D. Lawrence, and K. Q. Weinberger, editors, *Advances in Neural Information Processing Systems 27*, pages 2510–2518. Curran Associates, Inc., 2014.
- [22] Andre Wibisono, Ashia C. Wilson, and Michael I. Jordan. A variational perspective on accelerated methods in optimization. *Proc. Natl. Acad. Sci. USA*, 113(47):E7351–E7358, 2016.

APPENDIX A. AN IVP AS THE LIMIT OF THE PAGD METHOD

Here we derive the IVP (4.1) as a limiting case of PAGD.

A.1. Derivation of the ODE. Let us start with the same approach as in [21]. We assume, as an *ansatz*, that PAGD is a discretization of an ODE, which has a solution $X : [0, \infty) \rightarrow \mathbb{H}$, which we often call a *trajectory*. We also assume that X is smooth enough, e.g., twice continuously differentiable in time. In order to conveniently keep track of time variable, let us assume that $t = \sqrt{s}k$ always holds. That is, when the step size \sqrt{s} changes (e.g. when taking the limit $s \rightarrow 0$), the index k automatically changes along for $\sqrt{s}k$ to stay as close to t as possible and ignore the effect of the small mismatch of the two quantities. Another way of viewing this simplification is that we only look at the moments when the continuous time exactly agrees with the nodes of the time discretization. In short, the identifications such as $X(t) = x_k$, $X(t - \sqrt{s}) = x_{k-1}$, and $X(t + \sqrt{s}) = x_{k+1}$ will be made. For a fixed $t \in (0, \infty)$, the assumed smoothness on X , together with Taylor's formula in a normed vector space [11, Theorem 7.9-1] implies:

$$\begin{aligned} \frac{x_{k+1} - x_k}{\sqrt{s}} &= \dot{X}(t) + \frac{1}{2}\ddot{X}(t)\sqrt{s} + o(\sqrt{s}) \quad \text{as } s \rightarrow 0, \\ \frac{x_k - x_{k-1}}{\sqrt{s}} &= \dot{X}(t) - \frac{1}{2}\ddot{X}(t)\sqrt{s} + o(\sqrt{s}) \quad \text{as } s \rightarrow 0, \\ \text{(A.1)} \quad \sqrt{s}\mathcal{L}^{-1}G'(y_k) &= \sqrt{s}\mathcal{L}^{-1}G'(X(t)) + o(\sqrt{s}) \quad \text{as } s \rightarrow 0. \end{aligned}$$

The last identity follows from the continuity of G' , that of \mathcal{L}^{-1} , and (3.3), from which we can deduce $y_k \rightarrow X(t)$ as $s \rightarrow 0$. Substituting (3.3) into (3.2) and dividing by \sqrt{s} , we have

$$\text{(A.2)} \quad \frac{x_{k+1} - x_k}{\sqrt{s}} - \lambda \frac{x_k - x_{k-1}}{\sqrt{s}} + \sqrt{s}\mathcal{L}^{-1}G'(y_k) = 0.$$

Substituting the above Taylor expansions, and then rearranging, we arrive at

$$\text{(A.3)} \quad \frac{1}{2}(1 + \lambda)\ddot{X}(t) + \frac{1 - \lambda}{\sqrt{s}}\dot{X}(t) + \mathcal{L}^{-1}G'(X(t)) + o(1) = 0 \quad \text{as } s \rightarrow 0.$$

At this stage, the passage to the limit $s \rightarrow 0$ is not possible if λ is chosen independently of s . However, looking back at Algorithm 2, we see that the weight λ is actually a function of the step size \sqrt{s} . For the passage to the limit in (A.3) to be feasible, we must have $1 - \lambda = O(\sqrt{s})$ as $\sqrt{s} \rightarrow 0$. A faster rate of decay, $1 - \lambda = o(\sqrt{s})$ as $\sqrt{s} \rightarrow 0$, is possible. However, this leads to *frictionless* dynamics in the limit; see Remark 4.1. Since our physical intuition tells us that there is no hope of convergence in this case, we do not pursue this possibility. From this observation, we further assume that $(1 - \lambda)/\sqrt{s} \rightarrow 2\eta$ as $\sqrt{s} \rightarrow 0$ for some $\eta \in (0, \infty)$. Recalling Algorithm 2, and that $\lambda = \frac{1 - \sqrt{s}\sqrt{\mu}}{1 + \sqrt{s}\sqrt{\mu}}$, we have that $\eta = \sqrt{\mu}$. Letting $\sqrt{s} \rightarrow 0$, we obtain the following second order ODE:

$$\text{(A.4)} \quad \ddot{X}(t) + 2\eta\dot{X}(t) + \mathcal{L}^{-1}G'(X(t)) = 0.$$

A.2. Derivation of the initial conditions. The initialization $y_0 = x_0$ and (3.2) with $k = 0$ imply

$$\frac{x_1 - x_0}{\sqrt{s}} = \sqrt{s}\mathcal{L}^{-1}G'(x_0).$$

Take the limit $s \rightarrow 0$ and conclude $\dot{X}(0) = 0$ since G' and \dot{X} are assumed to be continuous. Therefore, we arrive at the desired IVP (4.1).

E-mail address, J.-H. Park: `jpark79@vols.utk.edu`

E-mail address, A.J. Salgado: `asalgad1@utk.edu`

E-mail address, S.M. Wise: `swise1@utk.edu`

DEPARTMENT OF MATHEMATICS, THE UNIVERSITY OF TENNESSEE, KNOXVILLE, TN 37996, USA